Available online at www.sciencedirect.com

SCIENCE DIRECT®

Tectonophysics 391 (2004) 35–65

TECTONOPHYSICS

www.elsevier.com/locate/tecto

Neotectonic evolution of the Anaximander Mountains at the junction of the Hellenic and Cyprus arcs

Johan H. ten Veen[a,*], John M. Woodside[a], Tiphaine A.C. Zitter[a,b], Jean F. Dumont[c], Jean Mascle[b], Anna Volkonskaia[d]

[a]*Centre for Marine Earth Sciences, Faculty of Earth and Life Sciences, Free University, De Boelelaan 1085, 1081 HV Amsterdam, The Netherlands*

[b]*Laboratoire de Géodynamique Sous-marine, Observatoire Océanologique de Villefranche, P.O. Box 48, 06230 Villefranche-sur-Mer, France*

[c]*UMR Géosciences Azur, Observatoire Océanologique de Villefranche-sur-Mer, P.O. Box 48, 06235 Villefranche-sur-Mer, France*

[d]*UNESCO–MSU Centre for Marine Geosciences, Faculty of Geology, Moscow State University, Vorobjevy Gory, Moscow 119899, Russia*

Accepted 3 June 2004
Available online 29 September 2004

Abstract

The Anaximander Mountains, occupying an outer-arc position at the junction of the Hellenic and Cyprus arcs, have been studied using a suite of geophysical data including multibeam swath bathymetry, backscatter images, seismic reflection profiles and gravity and magnetic data, which support an improved description of its deformation history. Lithologically, the western mountains can be correlated with the neritic limestones of the Bey Dağlari unit of SW Turkey. The eastern mountains relate to the ophiolitic Antalya Nappe Complex. In addition to this lithological contrast, a deep-seated crustal difference, which is best reflected in gravimetry, relates to the mid-Tortonian Aksu thrust phase. After the Early–Middle Miocene eastward emplacement of the Lycian Nappes, the Serravallian–Tortonian stage was characterized by the development of an array of grabens with N120°E strikes, which occupied a vast continental area that extended from southern Aegean to southwestern Turkey. During the mid-Tortonian, the last phase of thrusting marked the onset of a different kinematic regime related to the westward rotation of the Anatolian platelet. This Late Miocene change marked the start of differential subsidence that resulted in the formation of the Anaximander Mountains and which is reflected by an unconformity surface between the Lower–Middle Miocene and Plio–Quaternary units. The Messinian–Quaternary period in the western part of the Anaximander Mountains was characterized by distributed sinistral shear parallel to N70°E, which was marked by the onset of an extension on N20°E-striking normal faults that formed long graben-like depressions. During the Pliocene, these basins were transected by N70°E-striking sinistral strike-slip fault zones, although continued crustal extension suggests deformation in transtension. The eastern part of the Anaximander Mountains is instead characterized by N150°E-striking normal and/or oblique normal fault zones, which lack significant evidence of strike-slip deformation. Close examination of newly calculated predicted relative plate motions between Africa (from NUVEL-1A) and Anatolia (from GPS measurements) indicates that plate motion vectors change rapidly at the junction between the Hellenic and Cyprus arcs because of the close proximity to the pole of Anatolian rotation. These calculations indicate that along both the eastern Hellenic Arc and the western Cyprus arcs (the Florence Rise), the relative motion between

* Corresponding author. Tel.: +31 20 444 7365; fax: +31 20 444 9941.
E-mail address: johan.ten.veen@falw.vu.nl (J.H. ten Veen).

doi:10.1016/j.tecto.2004.07.007

the Anatolian and African plates is sinistral. On the southern Florence Rise, deformation is characterized by pure left-lateral faulting, whereas farther northwest, in the eastern Anaximander Mountains, the component of strike-slip decreases. Although arc-normal convergence predicts the occurrence of thrust faulting, southwestward trench retreat also causes an extension internal to this outer-arc domain, such that the preexisting N120°E-striking thrust faults of the Aksu phase have been reactivated as normal to oblique normal faults during the Pliocene and Quaternary. The observed sinistral faulting on faults striking N70°E in the western mountains is consistent with the relative plate motion along the eastern Hellenic Arc and merges with the extensional domain in the eastern mountains.

Keywords: Anaximander Mountains; Cyprus Arc; Hellenic Arc; Neotectonics; Eastern Mediterranean

1. Introduction

In its initial form, plate tectonics considered plate boundaries between converging plates to be approximately regular simple features, with a suite of kinematic domains that respond in a predictable manner to the subduction process. These concepts later changed, accepting that promontories, irregularities and obliquity of lithospheric convergence at active margins can play an important role in subduction-zone dynamics and may generate complex fault patterns (e.g., Molnar and Tapponier, 1975).

The Hellenic and Cyprus "double arc" system, evolving from the subduction of Africa beneath Eurasia, forms a good example of imminent continental collision governed by promontories and irregularities at the plate boundary. Several hypotheses exist as to how these arcs (Fig. 1) were once connected (Nur and Ben-Avraham, 1978; Rotstein and Kafka, 1982), originally forming an approximately east–west trending subduction zone (Le Pichon and Angelier, 1979). The subsequent segmentation of this originally E–W trending arc is believed to have been associated with several processes (in combination) including: (1) the Miocene closure of the Bitlis suture due to continental collision of the Arabian promontory of the African plate with Eurasia (Robertson, 1998) and the ensuing Pliocene–Recent westward extrusion of the Anatolian platelet into the Aegean domain (e.g., Taymaz et al., 1991; Le Pichon et al., 1995); (2) the subsequent onset of left-lateral faulting along the eastern Hellenic Arc (e.g., Huchon et al., 1982; Le Pichon et al., 1995; ten Veen and Meijer, 1998); and (3) the increasing curvature of the Hellenic Arc (e.g., Angelier et al., 1982; ten Veen and Kleinspehn, 2002). The effects of the extrusion of Anatolia are revealed by analogue modelling (Martinod et al., 2000), geomagnetic observations (e.g., Platzman et al., 1998) and geodetic measurements (e.g., McClusky et al., 2000).

Deep intraplate seismicity reveals active left-lateral faulting along the eastern Hellenic Arc (Papazachos et al., 2000), indicating that the strongly oblique plate convergence precludes active head-on subduction along this part of the arc. Active subduction beneath the Cyprus Arc appears to have stalled with the arrival of Eratosthenes Seamount at this subduction zone (Robertson, 1998). Along the western bend of the Cyprus Arc (the Florence Rise), most characteristics of subduction zones are lacking: there is no volcanic arc, no trench, no accretionary prism and low and dispersed seismicity (Ben-Avraham and Grasso, 1991; Woodside et al., 2002). Based on the observed structural pattern alone, Woodside et al. (2002) suggested that the Florence Rise is a transpressive right-lateral fault zone. This would suggest the existence of two oppositely shearing arc segments and the existence of complex strain patterns at the junction between the Hellenic and Cyprus arcs, consistent with both arcs increasing their convexity towards the south. The subducting slab is believed to be torn near the cusp between these arcs (Wortel and Spakman, 1992). Despite the significant increase in marine geophysical research in the eastern Mediterranean from the 1970s onward (Woodside, 1977), this junction between the Hellenic and Cyprus arcs has always been considered enigmatic as far as the relationship between subduction zone dynamics and observed crustal deformation is concerned.

This study describes new marine geophysical data from the Anaximander Mountains and surrounding areas, obtained during recent marine geophysical research (the TTR-1, ANAXIPROBE, TTR-6 and

MEDINAUT/MEDINETH projects). The dataset comprises a grid of seismic lines, complete EM12D multibeam echosounder bathymetry and imagery data, deep-tow sidescan sonar and subbottom profiler data, video images, gravity and magnetic data and extensive sampling from mud volcanoes and outcrops. Our aim is to accurately delineate and interpret the history of crustal deformation at the junction of the Hellenic and Cyprus arcs in order to come to better understand the dynamics of this subduction zone.

2. Data and methods

Most of the data presented in this paper were acquired during the two-part ANAXIPROBE cruise (1995 and 1996) which was focused on the Anaximander Mountains. The 1995 part provided multibeam bathymetry and backscatter images, seismic reflection profiles (see Fig. 1C for localities) and gravity and magnetic data. The seafloor bathymetry and backscatter were mapped using a Simrad EM12D multibeam echosounder system with 162 beams, providing 150° angular coverage over an ~15-km wide swath of seafloor centred beneath the ship. The seismic system comprised two GI 75 airguns (with a dominant frequency of 40–60 Hz), firing every 10 s, and a six-channel streamer, both towed at 7-m depth. The seismic data were collected using a Delphi (Ellics) system and processed using the computer program MSP Soft, including filtering with a band pass of 10/15–120/150 Hz. During the second part of the cruise, bottom samples were taken by dredging and gravity coring. High-resolution images of the seafloor texture were also obtained with a MAK-1 deep-tow system comprising a 30 kHz side-scan sonar and a 4.9 kHz subbottom profiler.

The 1998 PRISMED II expedition provided a similar dataset (i.e., Simrad EM12D multibeam bathymetry and backscatter images, seismic reflection profiles and gravity and magnetic data) which has already been used to study the Rhodes basin (Woodside et al., 2000) and the Florence Rise (Woodside et al., 2002) west of Cyprus (Fig. 1C).

In addition, we studied seismic reflection profiles from the 1991 TTR-1 (Training Through Research) cruise (Fig. 1C), which obliquely crossed the ANAXIPROBE seismic lines. For this cruise, the seismoacoustic source was a two-element 15 kJ sparker with a principal frequency band of 40–60 kHz and a 16-channel streamer. The grid-like arrangement of seismic lines obtained by combining the TTR-1 and ANAXIPROBE datasets enables us to trace structural features three-dimensionally.

3. Geological framework

The Anaximander Mountains (Fig. 1) are located at the junction of the Hellenic and Cyprus arcs and form an area of pronounced seafloor relief. They are bordered to the west by the deep Rhodes Basin (with depths up to 4485 m) and by the shallower (~2600 m) Antalya Basin to the east. This mountainous submerged region constitutes three distinctive mountains, Anaximander (*sensu stricto-s.s.*), Anaximenes and Anaxagoras (Fig. 2), next to several smaller culminations. The Anaximander Mountains *sensu lato* (*s.l.*) can be seen as the southernmost extent of the structurally complex Isparta Angle region (e.g., Blumenthal, 1963; Brunn et al., 1971) and are part of a broad zone of deformation defining the plate boundary.

Initially, the Anaximander Mountains were seen as upthrusted blocks of the Neotethyan seafloor that had been caught up in the collisional process (Ryan et al., 1973; Woodside, 1977). As an alternative, Nesteroff et al. (1977) interpreted these mountains as crustal blocks that had been separated from southwest Turkey during a post-Miocene collapse phase. Yet another view, by Rotstein and Ben-Avraham (1985), proposed that they were northward-colliding fragments of the African lithosphere which were caught up in the subduction process. More recently, the Anaximander Mountains have been shown to represent the offshore continuation of structural units exposed onshore in southwest Turkey (Woodside and Dumont, 1997). For instance, hydrocarbon seeps exist in both the eastern part of the Anaximander Mountains (Anaxagoras Mountain) and in the Antalya Nappe Complex (the eternal flames of Chimaera), suggesting a correlation between these terrains. This view is supported by extensive sampling of mud volcanoes and outcrops (Woodside et al., 1997) and by submersible observations (MEDINAUTH/MEDINETH Shipboard Scientific

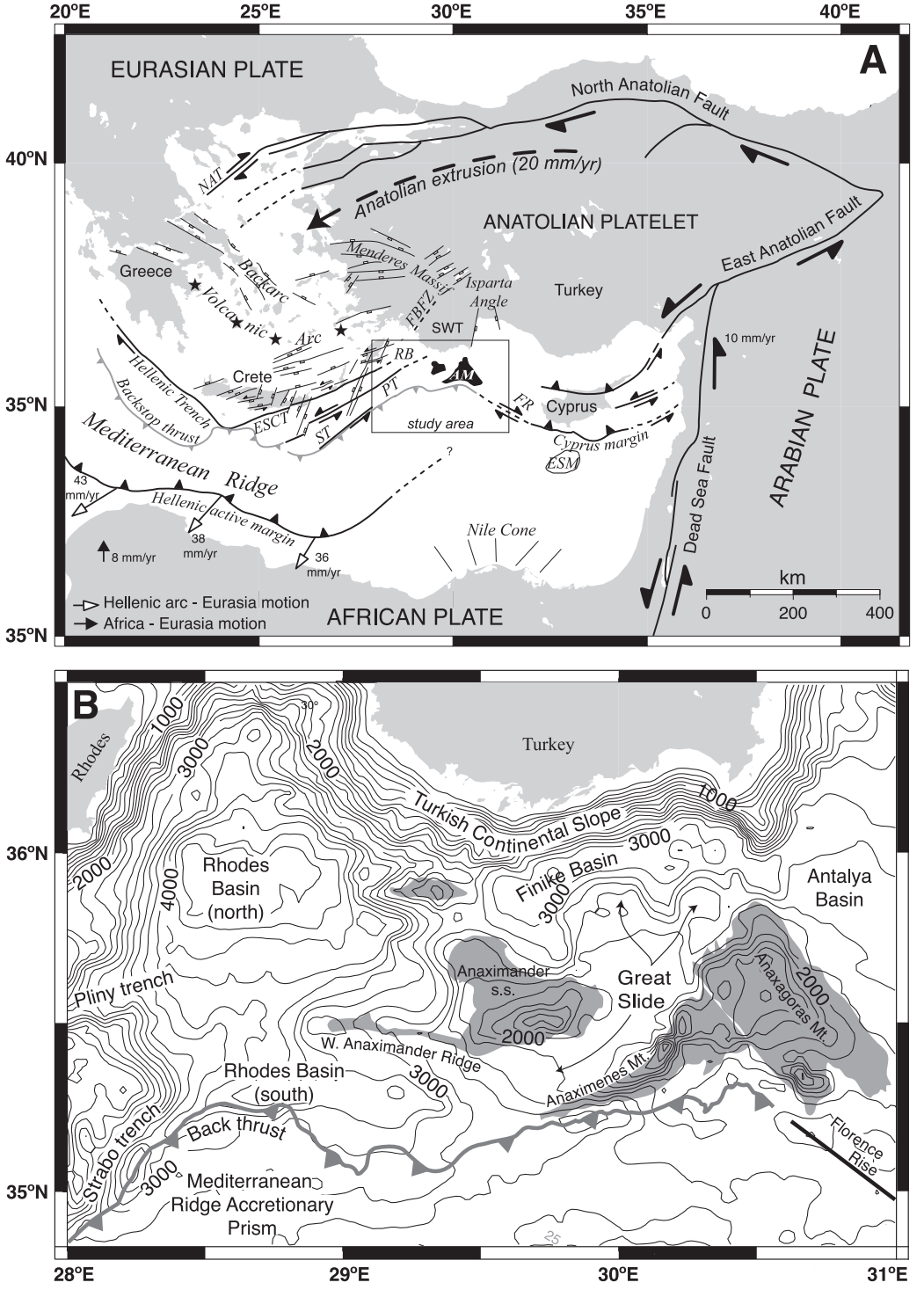
A
EURASIAN PLATE
North Anatolian Fault
Anatolian extrusion (20 mm/yr)
ANATOLIAN PLATELET
East Anatolian Fault
Greece
Turkey
Backarc
Volcanic Arc
Menderes Massif
Isparta Angle
FBFZ
SWT
RB
AM
PT
FR
Cyprus
Hellenic Trench
Backstop thrust
Crete
ESCT
ST
study area
Cyprus margin
ESM
Mediterranean Ridge
Hellenic active margin
43 mm/yr
38 mm/yr
36 mm/yr
8 mm/yr
Nile Cone
10 mm/yr
ARABIAN PLATE
Dead Sea Fault
km
0 200 400
Hellenic arc - Eurasia motion
Africa - Eurasia motion
AFRICAN PLATE
20°E 25°E 30°E 35°E 40°E
40°N
35°N
B
Rhodes
Turkey
Turkish Continental Slope
Rhodes Basin (north)
Finike Basin
Antalya Basin
Pliny trench
Anaximander s.s.
Great Slide
Anaxagoras Mt.
W. Anaximander Ridge
Anaximenes Mt.
Rhodes Basin (south)
Strabo trench
Back thrust
Mediterranean Ridge Accretionary Prism
Florence Rise
1000
2000
3000
4000
36°N
35°N
28°E 29°E 30°E 31°E

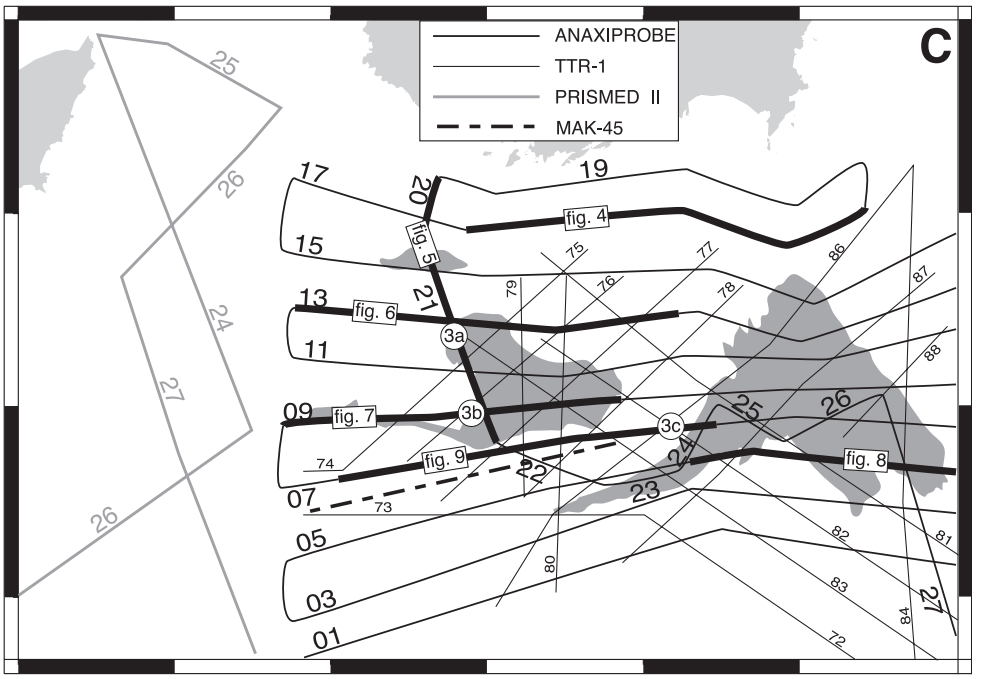

Fig. 1. (A) Geodynamic framework of the eastern Mediterranean. The motion vector of Africa is from DeMets et al. (1994) and the southwestward motion of the Hellenic Arc relative to Eurasia is from McClusky et al. (2000). The Hellenic forearc from Crete to Rhodes shows a strain pattern with N70°E-striking strike-slip faults and N20°E-striking normal faults, resulting from transtensional deformation since the Pliocene (ten Veen and Kleinspehn, 2002). The dextral shearing shown along the Florence Rise was inferred by Woodside et al. (2002). Our own results require the sense of shear in this locality to be sinistral instead. Abbreviations: ESCT=East South Cretan Trough; ST=Strabo Trench; PT=Pliny Trench; RB=Rhodes Basin; AM=Anaximander Mountains; FR=Florence Rise; ESM=Erastothenes Seamount; FBFZ=the hypothetical Fethiye–Burdur Fault Zone; SWT=Southwest Turkey; NAT=North Aegean Trough. Stars indicate subduction-related Quaternary volcanism. (B) Detail of the Anaximander Mountains study area with bathymetry from etopo5, made available through the National Geophysical Data Center (NGDC), with 200-m contour interval. Labels refer to structural domains that are discussed in text. (C) Seismic track lines of the ANAXIPROBE, TTR and PRISMED II cruises (after Woodside et al., 2000). Heavy line segments represent line segments illustrated in designated figure. Encircled numbers indicate parts of seismic lines shown in Fig. 3. MAK-45 indicates the deep-tow side-scan and subbottom profiler track shown in Fig. 10.

Parties, 2000). Dredge sampling has shown that the Turkish continental slope comprises neritic limestones similar to the Mesozoic Bey Dağlari Unit of SW Turkey. Flysch deposits are the most commonly observed rocks dredged from the Anaximander and Anaximenes mountains and from the SW part of the Anaxagoras Mountain. This offshore flysch unit most probably overlies the Bey Dağlari unit as it does onshore in SW Turkey, where it is derived from the leading edge of the Early–Middle Miocene advance of the Lycian nappes from the northwest (Hayward, 1984; Poisson et al., 1984). The NW–SE elongated Antalya orogen displays a wide variety of rock units including oceanic units (ophiolitic nappes), carbonate platform units and transitional (continental margin) units. The presence of ophiolitic rocks in the NE part of the Anaxagoras Mountain and in the continental slope southeast of Finike suggests a southward continuation of the Antalya Nappe Complex (Woodside and Dumont, 1997; Woodside et al., 1998). We are thus tempted to infer that the lithological contrast in the Anaxagoras Mountain is related to the mid-Tortonian Aksu thrust phase (Glover and Robertson, 1998) which emplaced the Antalya Nappe Complex westward onto the Bey Dağlari platform carbonates in SW Turkey (Poisson, 1977). This contrast is also shown by gravimetry, which reveals a major discontinuity in Bouguer gravity anomalies of 150 mGal between the Anaximenes and Anaximander mountains, with a maximum of 190 mGal, and eastern

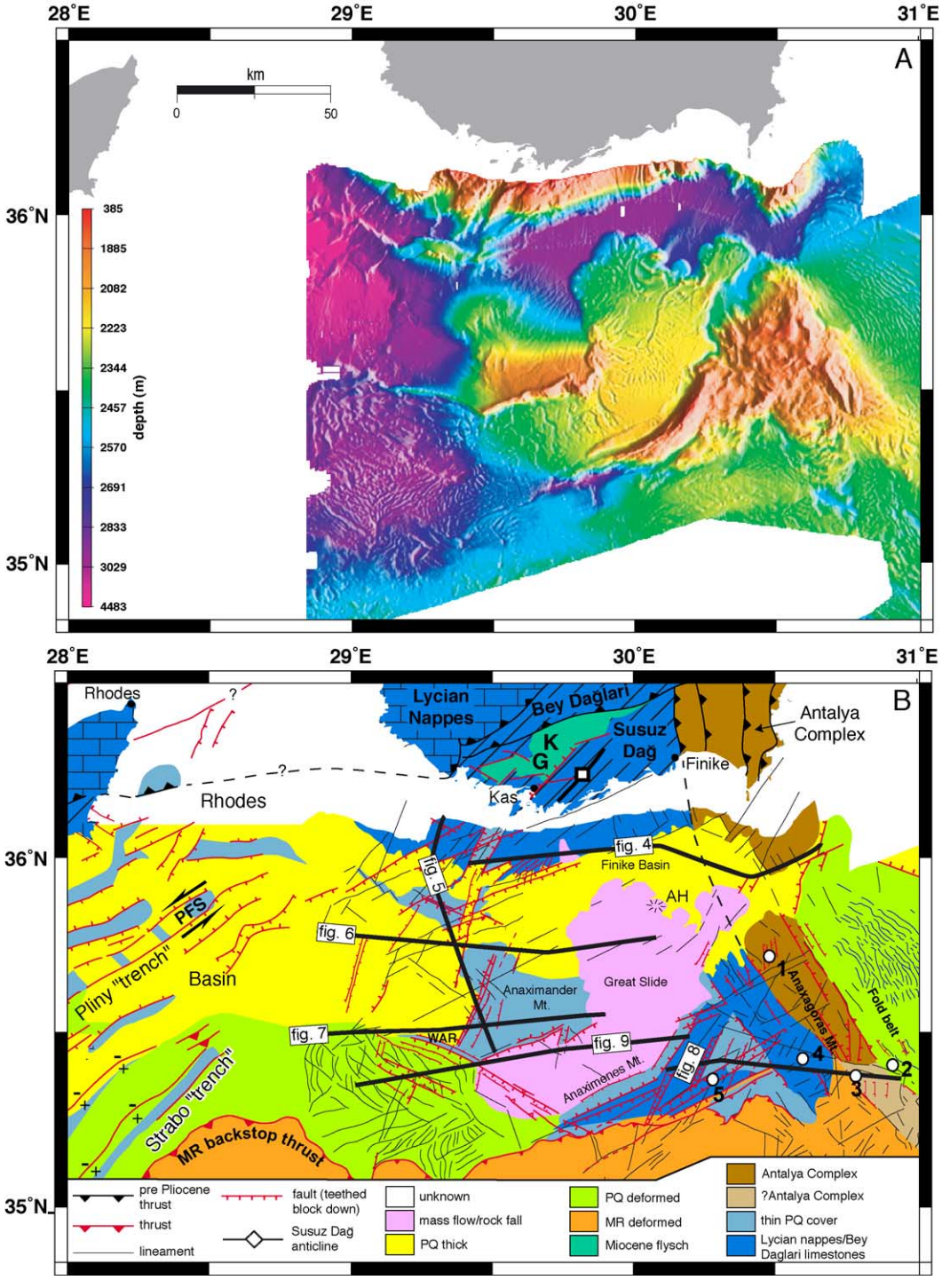
28°E
29°E
30°E
31°E
36°N
35°N
A
km
0
50
385
1885
2082
2223
2344
2457
2570
2691
2833
3029
4483
depth (m)
B
Rhodes
?
Lycian Nappes
Bey Daglari
K
G
Susuz Dag
Antalya Complex
Finike
Kas
fig. 4
Finike Basin
fig. 5
AH
fig. 6
PFS
Pliny "trench"
Basin
Anaximander Mt.
Great Slide
fig. 7
WAR
fig. 9
fig. 8
Anaxagoras Mt.
Fold belt
Anaximenes Mt.
Strabo "trench"
MR backstop thrust
1
2
3
4
5
pre Pliocene thrust
thrust
lineament
fault (teethed block down)
Susuz Dag anticline
unknown
mass flow/rock fall
PQ thick
PQ deformed
MR deformed
Miocene flysch
Antalya Complex
?Antalya Complex
thin PQ cover
Lycian nappes/Bey Daglari limestones

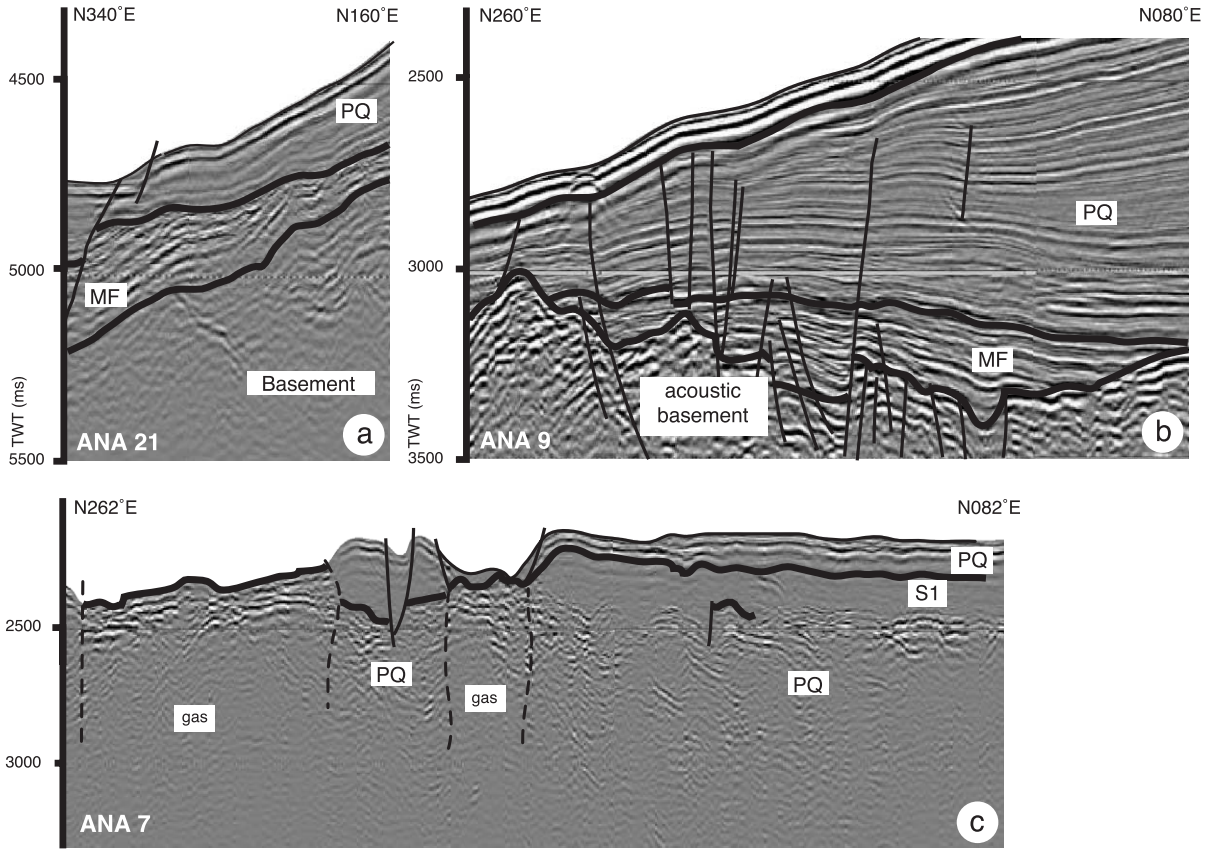

Fig. 3. Examples of seismic units. (a) Onlap of sedimentary unit MF onto acoustic basement. The younger unit PQ is separated from unit MF by an angular unconformity. (b) Detail of seismic line ANA9 showing infill of unit MF in a graben structure cut into a folded acoustic basement. This structure is covered by a thick (~400 m) sequence of tilted deposits of unit PQ. (c) Disturbance of seismic signal due to the presence of gassy sediments and possible gas vents. Low reflectivity unit represents slope deposits (unit S1) overlain by unit PQ.

Anaxagoras with a maximum of 40 mGal, which implies that the western mountains are undercompensated crustal blocks (Woodside, 1977; Ivanov et al., 1992; Zitter et al., 2003). However, the question remains whether the Aksu thrusting phase alone was responsible for these gravity anomalies or whether younger structures also contributed and will be the focus of this paper.

3.1. Basin fill and stratigraphy

The unconsolidated cover of the Anaximander Mountains and to a lesser extent the sedimentary fill of the adjacent basins have been studied with gravity coring (Woodside et al., 1997). With penetration depths up to ~5 m, it was demonstrated that the Upper Pleistocene–Holocene cover exists throughout

Fig. 2. (A) ANAXIPROBE multibeam bathymetry shown as colour-scaled shaded relief with illumination from the east (resolution is 10 m). (B) Interpretation of the Anaximander Mountains and the adjacent Rhodes Basin (from Woodside et al., 2000), showing in different colours the recognized structural domains. Heavy black lines indicate seismic lines shown in other figures. Faults (in red) signify high reliability structures that are recognized in both bathymetry and seismic lines (not all are shown). Lineaments (thin black lines) represent those (linear) features recognized in multibeam bathymetry alone. Generalized geology of southwestern Turkey is from Gutniç et al. (1979) and the Fethiye and Isparta sheets of the 1:250.000 Turkish Geological Map. See text for further explanation. AH=Anthill; KG=Kaşaba Graben. Mud volcanoes indicated by white circles: 1=Kula, 2=Saint Ouen l'Aumone, 3=Tuzlukush, 4=Kazan, 5=Amsterdam.

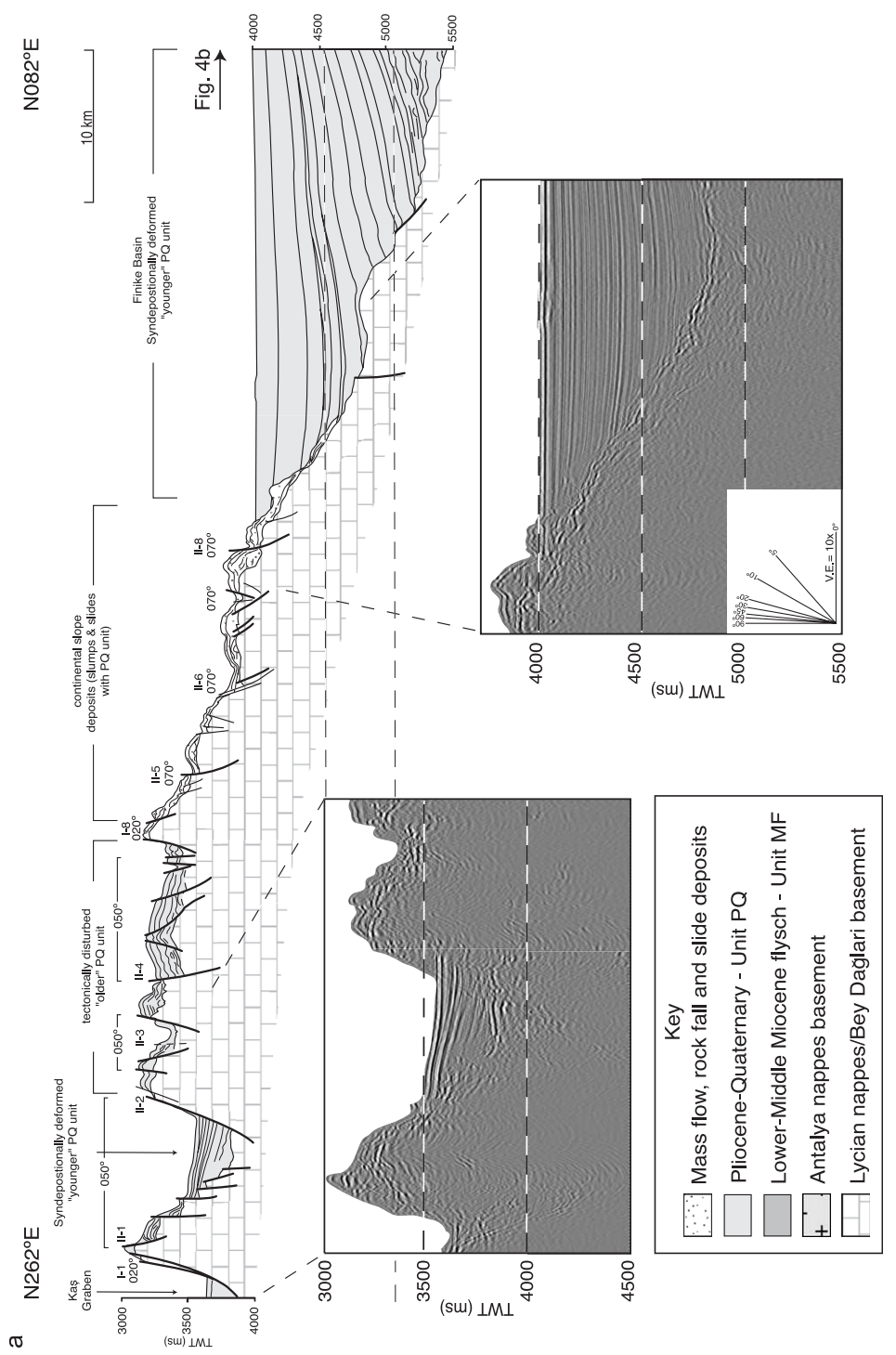
a
N262°E
N082°E
Kaş Graben
Syndepostionally deformed "younger" PQ unit
tectonically disturbed "older" PQ unit
continental slope deposits (slumps & slides with PQ unit)
Finike Basin Syndepostionally deformed "younger" PQ unit
10 km
Fig. 4b
I-1 020°
II-1 050°
II-2
II-3 050°
II-4 050°
I-8 020°
II-5 070°
II-6 070°
070°
II-8 070°
TWT (ms)
3000
3500
4000
4500
5000
5500
V.E. = 10x
Key
Mass flow, rock fall and slide deposits
Pliocene-Quaternary - Unit PQ
Lower-Middle Miocene flysch - Unit MF
Antalya nappes basement
Lycian nappes/Bey Dağlari basement

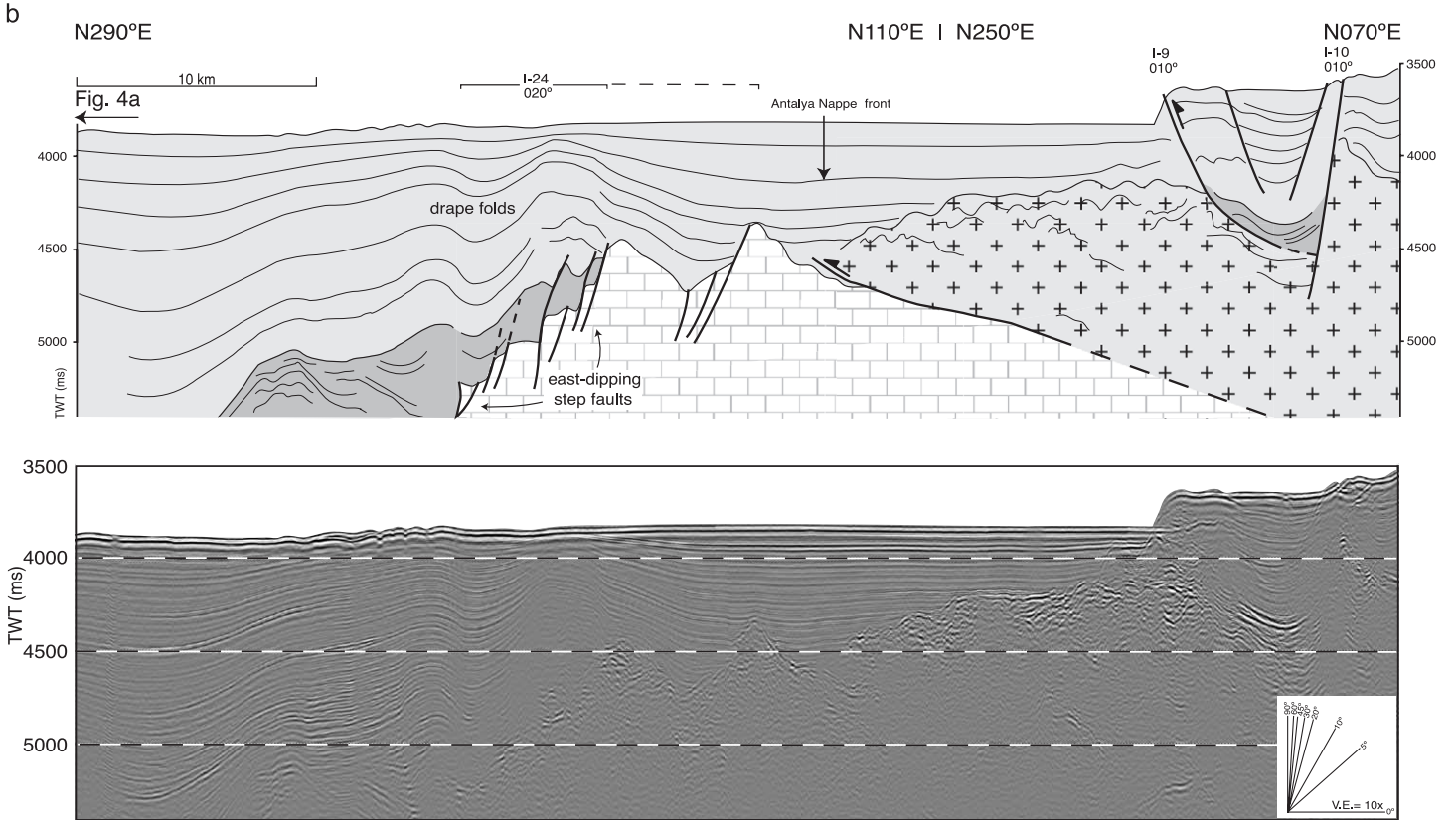

Fig. 4. Seismic line ANA17. Faults are labelled with their strike azimuths. (a) Section across the Turkish continental margin. (b) Section across the Finike Basin. See Fig. 1C or Fig. 2B for locations. Note 10 times vertical exaggeration.

the Anaximander Mountains. Many types of sediment, of different origins and depositional environments, were observed, reflecting the complex morphology, active crustal deformation and widespread fluid escape (Woodside et al., 1997). Several mud volcanoes were identified, with characteristic sedimentary features and associated mud breccias (Zitter et al., 2003). However, we will not focus on these surface deposits and will instead describe only those sediment types that are observable on the scale of seismic reflection profiles (i.e., representing seismic units):

(1) Deep marine unit PQ: this unit is present in the entire study area but dominates in its western part where it reaches a thickness of up to 1200 m. An angular unconformity exists between this unit PQ and the underlying unit (Fig. 3a and b). Unit PQ is further distinguishable by its draping appearance on the mountainous areas, whereas in some basins it shows reflectors dipping toward active faults (Fig. 4a). Next to Lower–Middle Miocene flysch, dredge samples from the Anaximenes Mountain reveal Lower Pliocene siltstones, indicating that unit PQ must represent a large part of the Pliocene–Recent period. Paleontological evidence from gravity cores suggests that unit PQ was deposited in a deep marine environment (Woodside et al., 1997), although no precise depth information exists for the parts that were not examined by gravity coring. Given that this unit was deposited after the mid-Tortonian Aksu phase and that no Messinian evaporites are encountered, its base may extend back into the Messinian as well.

(2) Flysch unit MF: this unit is only present west of the Anaximenes Mountain, is characterized by onlapping relationships with the acoustic basement and generally shows parallel internal reflectors that are sometimes wavy (Fig. 3a). Based on its stratigraphic position between the acoustic basement and the PQ unit, we assume that this unit MF corresponds to the Lower–Middle Miocene flysch deposits known from the Bey Dağlari in SW Turkey. In contrast with most other domains of the Mediterranean Sea, the "M" reflector that is related to the desiccation of the Mediterranean basin and the formation of evaporites during the Messinian (e.g., Ryan et al., 1973) is absent. This indicates that no deep marine basin existed in this area just prior to deposition of the Early Pliocene (PQ unit), similar to the situation in the presently deep marine Rhodes Basin (Woodside et al., 2000). We thus infer that the unconformity between the MF and PQ units formed sometime during the Late Miocene (Messinian) and signifies a period of vertical crustal motion and erosion controlled by the mid-Tortonian Aksu thrusting and the Messinian sea-level fall.

(3) Mass flow, rockfall and slope deposits (unit S): all deposits related to gravitational transport are assigned to this seismic unit, which appears as internally chaotic packages overlying the acoustic basement or the PQ unit (Figs. 3c and 4a, respectively). Slump and slide deposits in the Great Slide (Fig. 1B) are in turn overlain by younger hemipelagic sediments of unit PQ. Also, the chaotic rock fall deposits on the continental slope (Fig. 4a) are partly overlain by PQ deposits (Fig. 4).

4. Structure and morphology

4.1. The Turkish continental slope

The continental slope off SW Turkey has a steep gradient of 6–8° and is transected by numerous faults and scarps. Multibeam imagery (II-8 in Fig. 2) shows several N70°E-trending lineaments, the most important of which is located at the slope break. The N20°E-striking graben (valley) south of Kaş, hereafter designated as the "Kaş Graben", forms an important discontinuity in this continental slope. To the north, this graben is continuous with the onshore Kaşaba Graben in the Susuz Dağ, which postdates the Middle Miocene as it preserves the originally widespread Miocene flysch deposits (see Hayward, 1984). Our preliminary fieldwork shows that the Kaşaba Graben is cut by a series of N70°E-striking oblique normal faults which have displaced the boundary faults of this graben left-laterally by up to several tens of metres.

The high-resolution bathymetry in combination with crossing seismic lines ANA-17 and ANA20-21

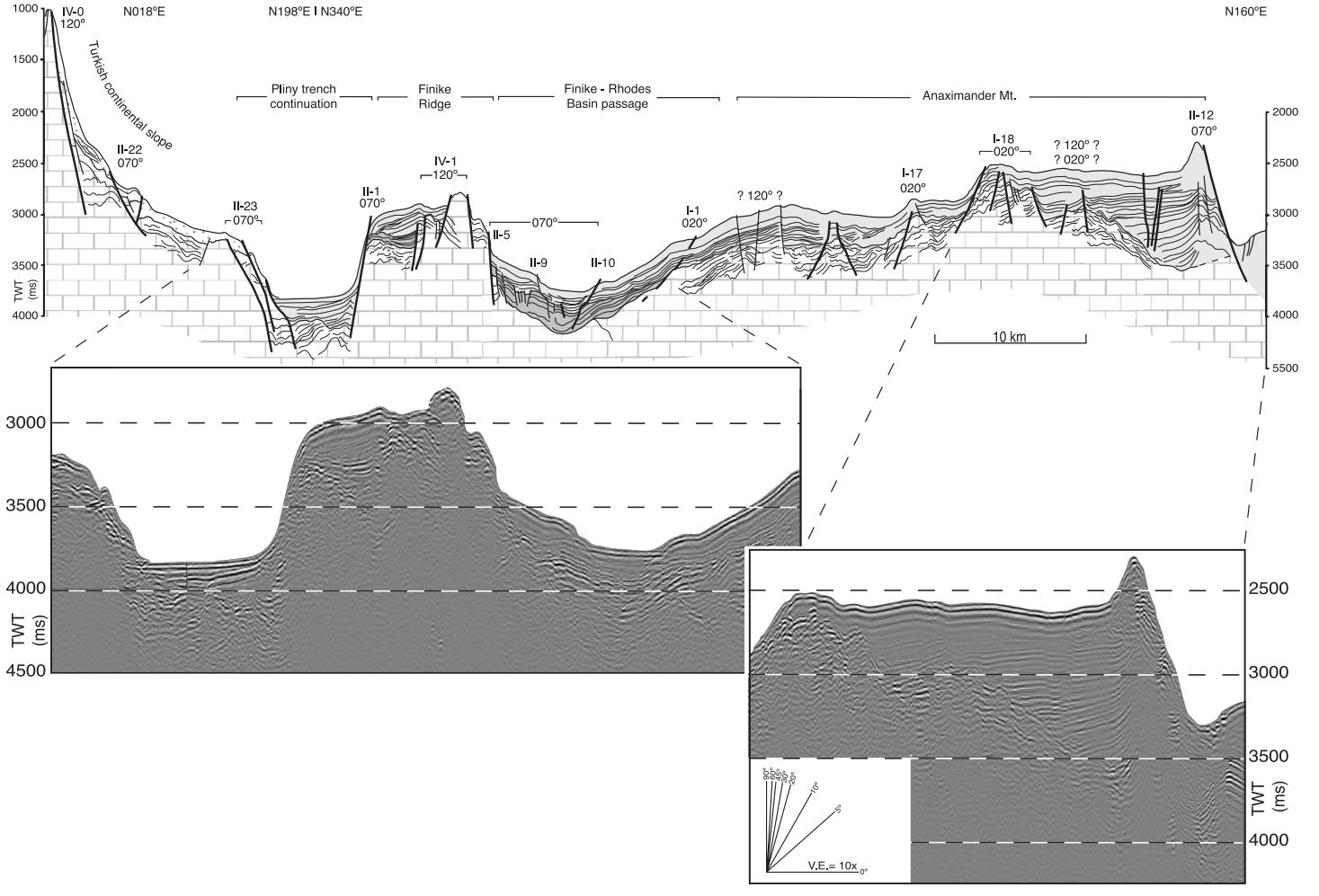

Fig. 5. Seismic line ANA20-21 in an N–S transect from the Turkish continental margin to the Anaximander Mountain *s.s.* Faults are labelled with their strike azimuths. See Fig. 1C or Fig. 2B for location and Fig. 4a for key.

(Figs. 4 and 5) enables recognition of the orientation of many morphology-related faults. ANA-17 reveals how, east of the Kaş Graben, the continental slope is cut by a series of N50°E- and N70°E-striking faults (II-5–II-8 in Fig. 4a). The lineament patterns observed in the multibeam bathymetry (Fig. 2B) suggest that the N50°E-striking linear features are delimited by the N70°E-striking ones. Because the N50°E-striking faults are relatively small and are not observed elsewhere in the Anaximander Mountains, we speculate that they are not only confined by but also associated with the N70°E-striking faults. If the N70°E-striking faults represent principal sinistral strike-slip faults, the N50°E-striking faults may represent synthetic (Riedel shear) faults. However, the tectonic disturbance and displacement of unit PQ only indicate a strong dip-slip component for the N50°E-striking faults (Fig. 4a). The lower continental slope is covered by an acoustically chaotic unit, which corresponds to an area with strong contrasting (patchy) backscatter, which we interpret as a rockslide (see Fig. 2 for location). Southeast of the continental slope (i.e., in the Finike Basin), only minor faults exist. The fill of this basin appears to be progressively tilted, with older strata dipping more steeply than younger strata. This may indicate syn-depositional tilting in response to slip on the N70°E-striking basin-bounding faults (Fig. 4a).

Farther east, the thick basin fill of the Finike Basin comprises folds with wavelengths of several kilometres (Fig. 4b). These folds occur west of a major thrust fault beneath the chaotically deformed acoustic basement that we relate to the Aksu thrusting phase. Similar to the distribution of basement units onshore and based on observations from the Anaxagoras Mountain, we infer that this acoustic basement represents the thrust front of the Antalya Nappe Complex (see also Fig. 2). In the Anaxagoras Mountain, this thrust front is obscured by a N150°E-striking (i.e., S030°E-striking) fault zone that forms the present-day contact between the Antalya Nappe Complex and the acoustic basement exposed to the west (Fig. 2). Because no folds occur just in front of or above the Antalya nappe front, we suggest that the folds observed in the Finike Basin are not directly related to thrusting but represent drag or drape folds above faulted or collapsed acoustic basement.

In a transect perpendicular to the continental slope (Fig. 5), it becomes further clear how faults of different orientations are responsible for the morphology of this slope. An N120°E-striking fault (IV-0) forms the main step in this slope but abuts eastward against the N20°E-striking Kaş Graben (Fig. 2). To the south, this N120°E-striking fault is delimited by a series of N70°E-striking faults that constitute a graben-like depression. The acoustic basement high south of this depression, the Finike Ridge, is transected by N130°E-striking faults but is bounded by N70°E-striking faults. This, together with uplifted PQ unit, suggests an inversion of an older N120°E-trending basin by slip on N70°E-striking faults. On the uplifted block, the older MF unit is unconformably overlain by the PQ deposits. We thus speculate that this basement high forms the uplifted crest of a tilted footwall block of a N120°E-trending graben which preserves these older deposits. This graben was then later cut by N70°E-striking faults, causing differential uplift and deformation of both the MF and PQ deposits, confining the age of the N70°E-striking faulting to the PQ and younger period. To the west of this zone of uplift, N120°E-trending ridges appear to be sinistrally displaced by N70°E-striking faults with horizontal components of slip of up to 2 km (Fig. 2), confirming both the sinistral slip sense of the N70°E-striking faults and the proposed sequence of faulting.

4.2. Anaximander Mountain *s.s*.

The Anaximander Mountain *s.s*. is the westernmost submarine mountain of the studied area; it has a gently sloping (2°) northward facing leeside and a steeply dipping (13°) south-facing slope. This leeside is marked by closely spaced channels that are oriented downhill (i.e., to the north; Fig. 2A). Upslope (i.e., southward), these channels bend to a more E–W orientation, suggesting that downhill transport towards the Finike basin has been governed by recent differential vertical movements that have changed the leeside slope direction.

Line ANA20-21 (Fig. 5) covers the entire northern slope of the Anaximander Mountain *s.s*., which marks the transition to a narrow basin that defines the connection between the Rhodes Basin and the

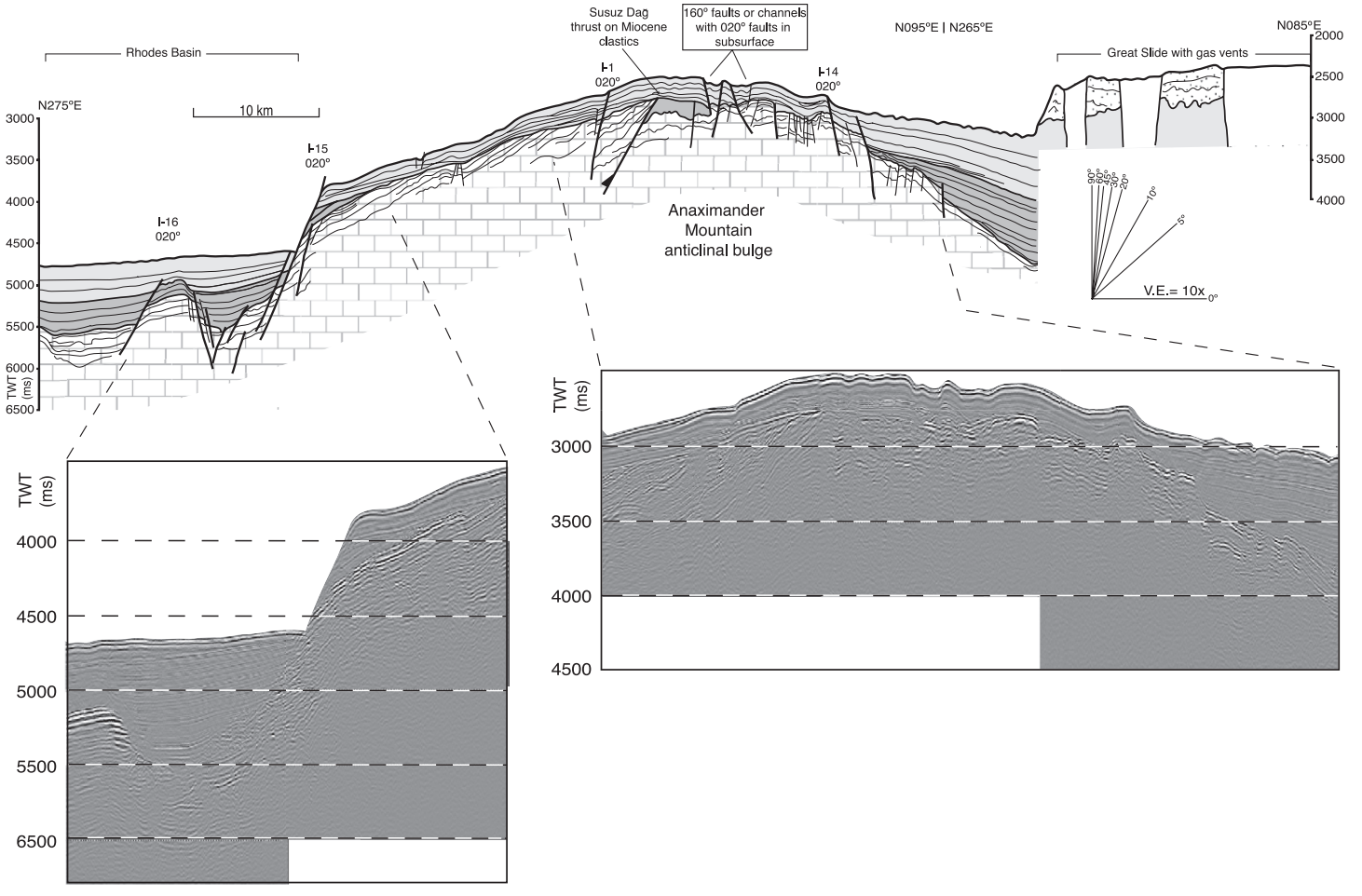

Fig. 6. Section of seismic line ANA13 showing an approximately E–W transect across the Anaximander Mountain *s.s.* and the Great Slide. Faults are labelled with their strike azimuths. See Fig. 1C or Fig. 2B for location and Fig. 4a for key.

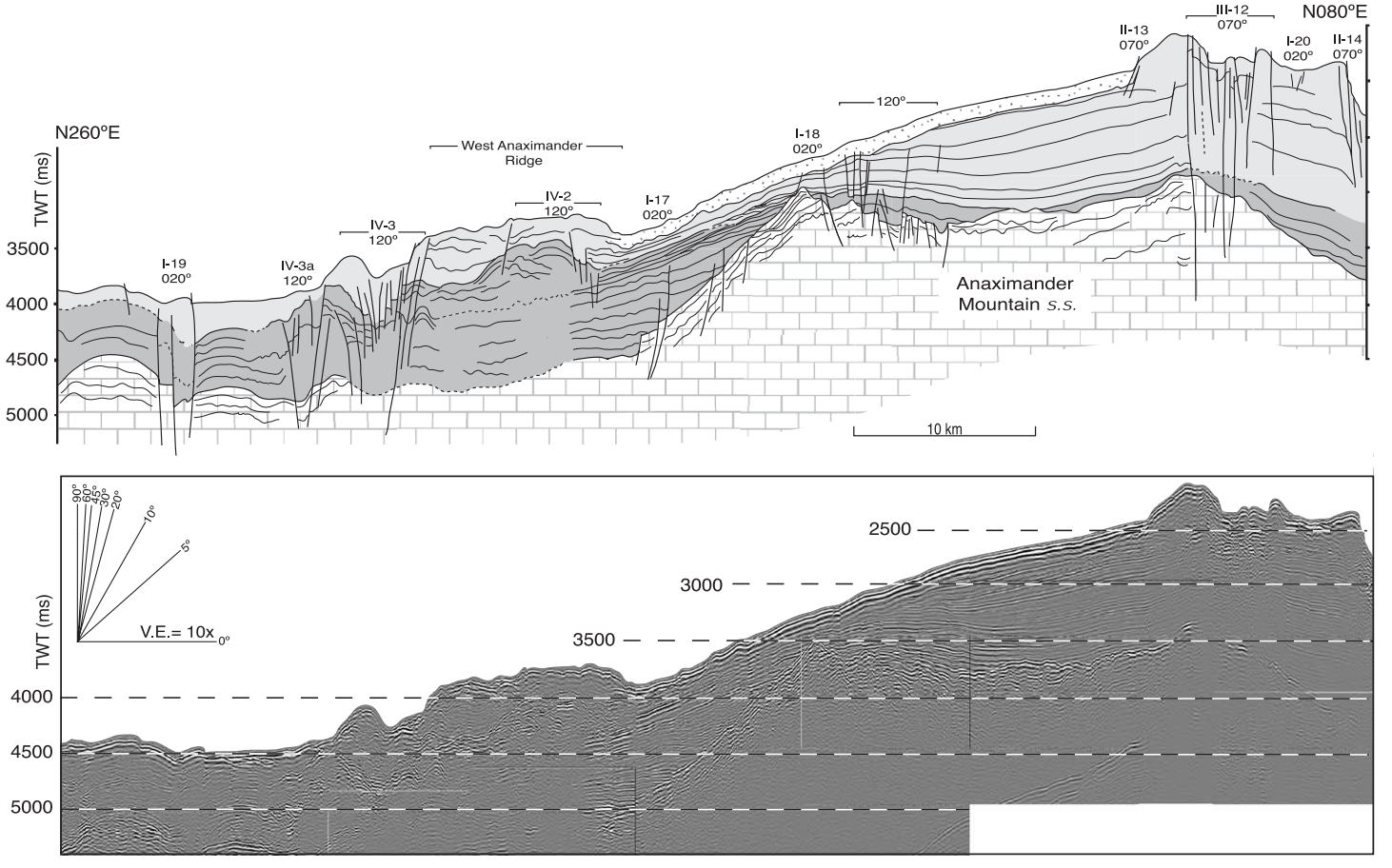

Fig. 7. Section of seismic line ANA9 in an approximately E–W transect across the West Anaximander Ridge and Anaximander Mountain *s.s*. Faults are labelled with their strike azimuths. See Fig. 1C or Fig. 2B for location and Fig. 4a for key.

Finike Basin. This Rhodes–Finike passage is controlled and bounded by N70°E-striking faults (Figs. 2 and 5) that clearly affected the seafloor relief, suggesting a relatively young age for this passage. The sedimentary sequence in this Rhodes–Finike passage began with seismic unit MF, which laps onto the Anaximander Mountain *s.s.* to the south and is unconformably overlain by the draping unit PQ. Line ANA13 (Fig. 6) crosses the Anaximander Mountain *s.s*. from east to west and shows that this mountain is delineated to the west by a major N20°E-striking normal fault (I-15) that vertically displaced both units MF and PQ by up to ~600 m. On both lines, ANA20-21 and ANA13 (Figs. 5 and 6), a bulge-like structure is visible, which is onlapped by unit MF from the east, north and west. Here, unit MF is erosionally truncated beneath the angular unconformity with the overlying draped PQ unit. This relationship indicates that this bulge must have been present during the Early–Middle Miocene deposition of unit MF but was elevated further and eroded prior to deposition of unit PQ, possibly through a combination of the mid-Tortonian Aksu phase and the Messinian sea-level fall. This suggested timing of formation of this bulge corresponds with that of the onshore Susuz Dağ anticline in SW Turkey (Fig. 2B). Farther south, the seafloor rises steeply and the bulge-like geometry is strongly affected by several N20°E-striking step faults (notably, I-17 and I-18 in Fig. 5) which form horst and graben structures. South and east of this horst, the acoustic basement deepens and the PQ unit thickens rapidly (Figs. 6 and 7). The summit of the Anaximander Mountain is formed by the thickest sequence of PQ deposits, which are uplifted and folded along the N70°E-trending fault zone (II-12; right hand end of Fig. 5), suggesting that this is a relatively young structure (in relatively unstable unlithified sediment) that has not yet been eroded.

The Anaximander Mountain *s.s.* thus developed as a result of the interaction of N20°E- and N70°E-striking faults bounding an existent anticlinal bulge, with the most important bathymetric offset at its southern edge, determined by fault II-12 (Figs. 5 and 7). Some N130°E-trending lineaments in the bathymetric image in Fig. 2 can be associated with faults, but judging by their displacements, they are of minor recent importance.

4.3. Anaximenes Mountain

The Anaximenes Mountain is an elongated, curved mountain range bounding the Great Slide to the south and east. Its steep northern slope (sloping at 18° in the south, increasing to 24° in the north) appears smooth on the multibeam imagery (Fig. 2A). However, closer examination of both seismics and lineament patterns reveals that this slope is controlled by faults of different orientations. Its southern NE–SW trending part is bounded and transected by N70°E-striking faults, whereas its northern part is delineated by N20°E-striking faults. The gently sloping (7°) southeastern slope of the Anaximenes Mountain (Figs. 8 and 9) is made up of a series of N20°E-striking step faults with associated down-faulted blocks. Two broad (up to 3-km wide) N50°E–N60°E-trending shear zones (II-18 and II-19) cross this side of the Anaximenes Mountain and also cross cut the N20°E-striking fault zones (Fig. 2). Locally, the PQ sediment occurs in patches, which seem to be confined to fault-controlled depressions. Some of the larger N70°E-striking fault zones can be traced as far as the Anaxagoras Mountain, but the N20°E-striking fault zones abut against the N150°E-trending western boundary faults of this mountain (Fig. 2B). This arrangement suggests that the N20°E-striking faults are older than the N150°E-striking faults that cross and delineate the Anaxagoras Mountain and that the N70°E-striking faults are thus the youngest structural features. The southern boundary of the Anaximenes Mountain is formed by a N70°E-striking fault zone (II-19) which connects westward to a deep trough separating this mountain from the relatively flat Mediterranean Ridge region (MR in Fig. 2). The Amsterdam mud volcano at the SE edge of the Anaximenes Mountain is situated in this N70°E-striking fault zone, which includes many associated smaller-scale faults that belong to the N70°E-, N20°E- and S60°E-striking fault groups.

4.4. Anaxagoras Mountain

Seismic lines across the Anaxagoras Mountain support the assumption that this mountain is an elevated part of the Florence Rise, defined by NW–SE-striking faults and cut by several NE–SW-striking faults (Woodside et al., 2002; Zitter et al., 2003).

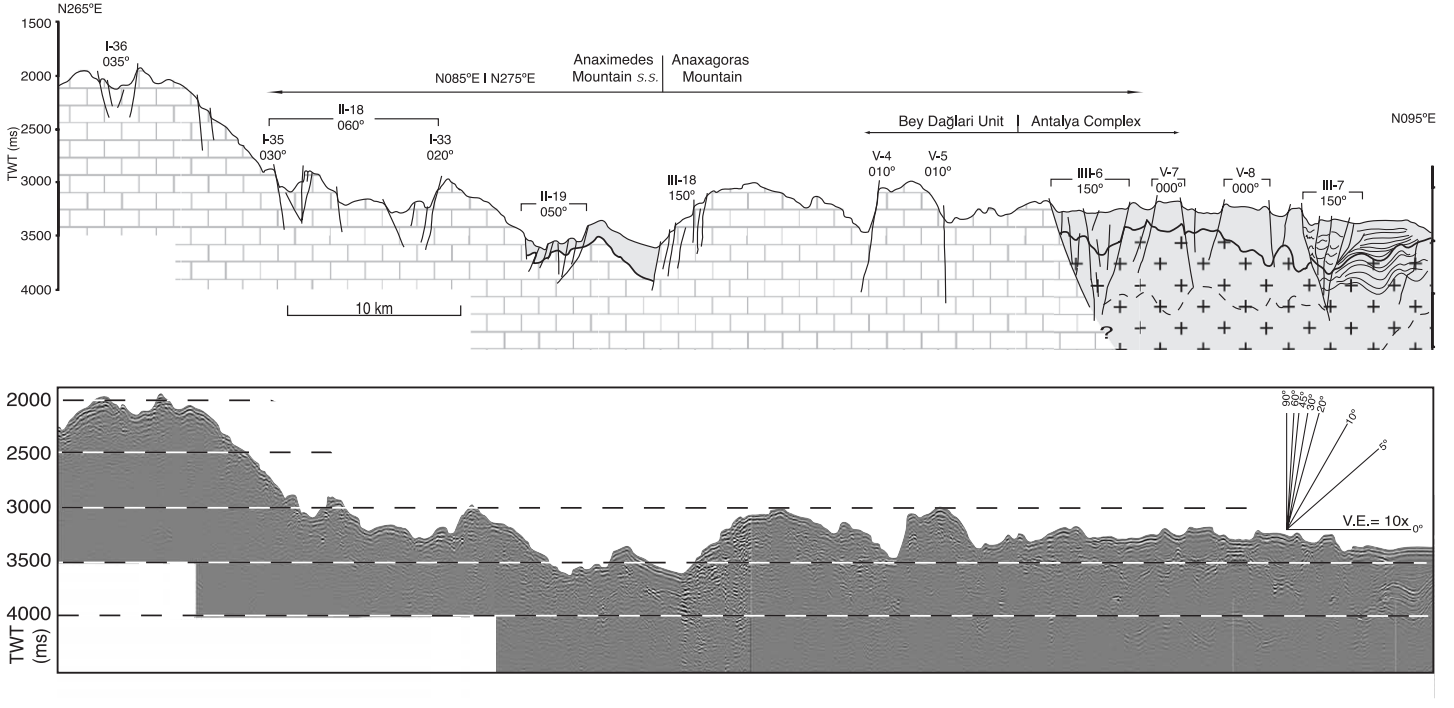

Fig. 8. Section of seismic line ANA5 in an approximately E–W transect from the Anaximenes Mountain towards the Anaxagoras Mountain *s.s.* Faults are labelled with their strike azimuths. See Fig. 1C or Fig. 2B for location and Fig. 4a for key.

Whereas the western mountains are dominated by N70°E- and N20°E-striking faults, the Anaxagoras Mountain is dominated (bounded and transected) by N150°E-striking faults, although some of the larger N70°E-striking faults zones also cross it (Fig. 2). One important N70°E-trending lineament follows a NE–SW-oriented ridge, the "Faulted Ridge", along which the bathymetry is displaced in a sinistral sense (Woodside et al., 1997). Although a few N20°E bathymetric trends can be recognized in the Anaxagoras Mountain, no faults related to these appear in the seismic lines. These N150°E-striking faults do not occur in the Anaximander *s.s.* and Anaximenes Mountains.

Several N–S lineaments in the bathymetry of the Anaxagoras Mountain can be interpreted as normal faults from their dominant components of dip-slip and relatively simple fault geometries. These faults are short (<10 km), their length being limited by more complex N120°E-striking fault zones, as is demonstrated by faults V-7 and V-8 in Fig. 8. This arrangement suggests that the N–S faults are either recently reactivated older faults or young extensional faults that have an unknown association with the N120°E-striking faults. In cross-section (Fig. 8), these N120°E-striking faults appear to be relatively young, as they cut through the Pliocene–Quaternary cover and exhibit negative flower structures that create minor bathymetric steps. However, a strike-slip origin for them is hard to establish as there are no signs of horizontal displacement. This led us to conclude that these N120°E-striking faults accommodate oblique slip, with complex geometries that may indicate some strike-slip, but with an unknown sense of lateral slip.

The Kula mud volcano (Fig. 2B) is also marked by relatively short N–S- to N10°E-striking faults that act as conduits for the mud ejection. However, not all mud volcanoes are associated with the same orientation of faults and fissures. For example, the Kazan mud volcano (Fig. 2B) is transected by at least six fault orientations, suggesting complex deformation at the junction of major N70°E- and N120°E-striking fault zones (due to its location at the contact between the Anaximenes and Anaxagoras mountains). The Tuzlukush and Saint Ouen l'Aumône mud volcanoes, on the southern edge of the Anaxagoras Mountain (Fig. 2B), are also associated with N70°E- and N120°E-striking faults. All these mud volcanoes have N120°E-trending fissures that are of minor importance relative to other orientations.

The Antalya Basin, east of the Anaxagoras Mountain, is characterized by subparallel, anastomising ridges that curve from an N120°E strike in the north to N160°E in the south (Fig. 2) and have the appearance of a fold belt. To the northeast, this fold belt is delimited by an ~N120°E-striking fault with a vertical offset of ~1250 m down to the northeast as concluded from the easternmost part of ANAXIPROBE seismic line 15 (Zitter et al., 2003; not shown in figure) This fault separates the fold belt, which has up to 800 m of Plio–Quaternary sediment, and the deep Antalya Basin with a thickness of more than 1700 m. The anastomising ridges rise up to ~100 m above the surrounding seafloor and appear related to folds in the subrecent sediment (unit PQ). This morphological pattern seems to argue against faulting as the main cause for the development of this structural domain, although a series of (presumably subparallel-trending) west-dipping step faults occurs in the subsurface (Fig. 4b) This combination of folding above a strongly folded and possibly faulted substratum may indicate halokinesis of Messinian evaporates, which are widely present in the Antalya Basin (Biju-Duval et al., 1974; Woodside, 1977; Sage and Letouzey, 1990).

4.5. Southeastern Rhodes Basin

The Rhodes Basin, one of the deepest Mediterranean basins (up to 4485 m), has probably formed as a result of the progressive development of transform motions along the eastern branch of the Hellenic Arc during the Pliocene and Quaternary periods (Woodside et al., 2000). The Rhodes Basin consists of two subbasins, a northern deeper one and a shallower southern one, separated by a broad asymmetrical swell oriented roughly east–west. The southern Rhodes Basin is confined by the West Anaximander Ridge to the north, the Mediterranean Ridge accretionary prism to the south and the Anaximander Mountains to the east (Fig. 1). The intense deformation in this domain is reflected by the undulating seafloor topography (Fig. 2A). Whereas the Anaximander Mountain *s.s.* is dominated by N20°E-striking normal faults and N70°E-striking sinistral strike-slip faults, the SE Rhodes Basin dominantly comprises

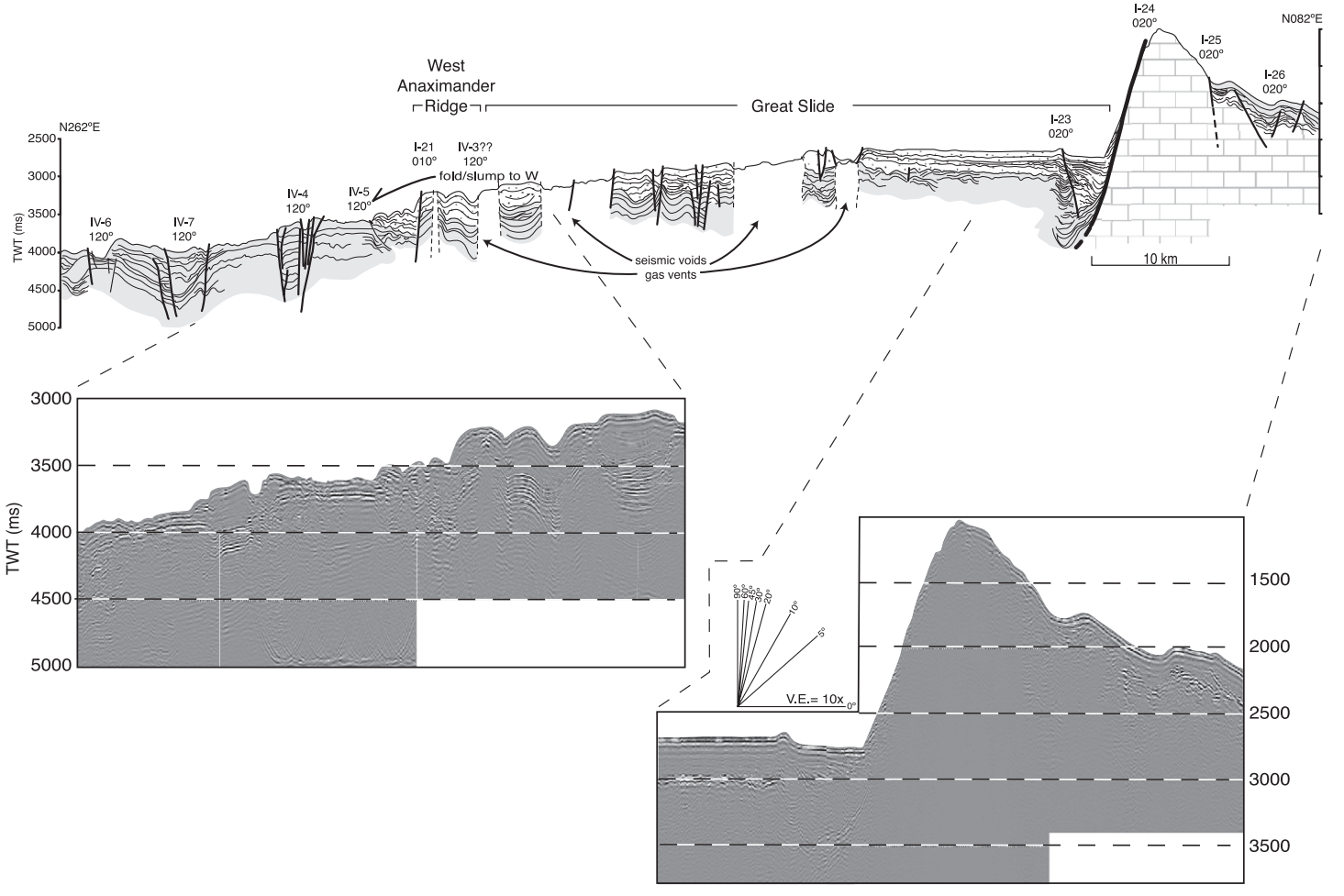

Fig. 9. Section of seismic line ANA7 in a approximately E–W transect from the southeastern Rhodes basin across the Great Slide and Anaximenes Mountain. Faults are labelled with their strike azimuths. See Fig. 1C or Fig. 2B for location and Fig. 4a for key.

N120°E-trending fault zones. This transition, at the western side of the Anaximander Mountain *s.s*, is marked by the West Anaximander Ridge, a pronounced but narrow N120°E-trending ridge that dies out westward in the deepest, central part of the Rhodes Basin (Fig. 1). This ridge is bounded to the north by N120°E-striking fault zone IV-2 and to the south by fault zone IV-3 that is ~3- to 4-km wide, has a clear negative flower structure (Fig. 7) and includes many individual smaller faults. Fault zone IV-3 can be traced southeastward for more than 100 km and constitutes the SW limit of the Anaximenes Mountain (Fig. 2). The appearance of this fault zone varies along strike and includes segments with either negative or positive flower structures, although the degree of deformation typically decreases southward. South of this fault zone, several other less important N120°E-striking faults zones exist, which also have flower-like structures (e.g., IV-4, IV-6 and IV-7 in Fig. 9). The observed along-strike variations in deformation styles and the presence of flower structures and anastamosing fault traces suggest that these N120°E-striking faults take up strike slip. Multibeam imagery suggests that the areas between these pronounced N120°E-striking fault zones comprise NNW–SSE trending depressions, which we interpret as small pull-apart basins. This association of structures implies that these N120°E-striking faults have a dextral slip component. Although N120°E-striking faults dominate just south of the West Anaximander Ridge, farther south N70°E-trending lineaments can instead be seen in the multibeam imagery. These bound zones with NNW–SSE trending depressions, which may also represent pull-apart structures and which strengthen the interpretation of sinistral strike-slip character of the N70°E-striking faults. However, side-scan sonar images of this region indicate that many of these linear features are caused by superficial deformation related to sediment movement. This seemingly organized structural pattern may indicate that this superficial sediment deformation reflects regional-scale deeper-seated crustal deformation.

Some N20°E-striking normal faults in the southern Rhodes Basin delineate horst structures that are partly buried by the PQ unit (Fig. 6). The fact that the N120°E-striking faults in this locality are more clearly related to seafloor morphology suggests that they are younger than the N20°E-striking faults. The presence of some N120°E-striking faults in the Anaximander Mountain *s.s.* and in the Turkish continental slope (Fig. 5), which are older than the N20°E- and N70°E-striking faults, may indicate that this fault set in the southern Rhodes Basin represents reactivated older structures. Although correlation across such a great distance may seem optimistic, the West Anaximander Ridge does correlate across the Rhodes Basin with subparallel fault zones on Rhodes island (see Fig. 15 of ten Veen and Kleinspehn, 2002), suggesting genetically related deformation. These N120°E–N130°E-striking normal faults originated in the Middle–Late Miocene (Serravallian–Tortonian) in response to NE–SW extension and in several cases were reactivated during younger deformation phases (ten Veen and Kleinspehn, 2002).

The southern edge of the Rhodes Basin is formed by the contact with northward-directed (sediment) nappes of the Mediterranean Ridge and lies in continuity with the Strabo Trench as was first noted by Mascle et al. (1986). This irregular thrust front can be traced eastward where it merges with N70°E-striking strike-slip faults south of the Anaximenes Mountain.

4.6. Northern Rhodes Basin

The asymmetric swell that separates the northern and southern parts of the Rhodes Basin marks an important change in the degree of deformation, with more strongly deformed acoustic basement to the north (Woodside et al., 2000). Closer examination of the data presented by Woodside et al. (2000) reveals that this E–W swell connects the N120°E-trending West Anaximander Ridge and a N70°E-trending transpression-related bathymetric swell north of the Strabo Trench. In the central Rhodes Basin, a positive flower structure has been identified (PFS in Fig. 2B; Woodside et al., 2000), which coincides with the broad and complex Pliny "trench". Together with its N70°E-trending linear morphology and en échelon subbasins, this suggests that the Pliny "trench" has accommodated post-Miocene sinistral slip (Huchon et al., 1982; Le Pichon et al., 1995). Both faults and bathymetric trends associated with the Pliny "trench" in the Rhodes basin link with N70°E-striking faults in the Turkish continental slope, which delineate the Finike Basin (Fig. 2), suggesting that this Plio–

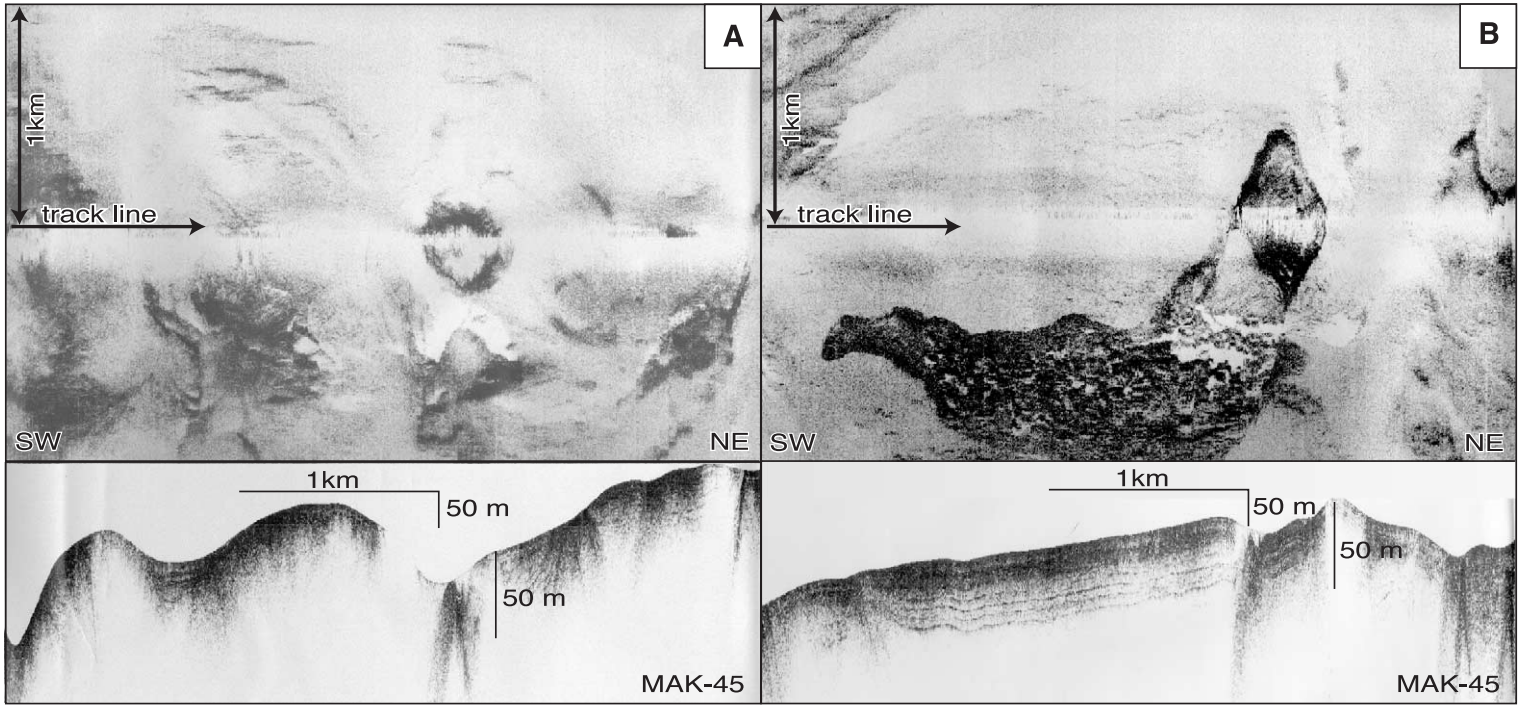

Fig. 10. MAK-45 deep-tow side scan sonar image (top) and subbottom profiler image (bottom) of some features associated with the Great Slide. For locality see Fig. 1C. (A) Circular pock marks above seismic voids that are possibly related to the presence of gassy sediments and/or gas vents. (B) Southwestward flowing slump body with slump scar.

Quaternary basin is the continuation of the Pliny "trench". This interpretation, strongly supported by the marine geophysical data presented here, precludes an alternative interpretation in which the Pliny "trench" is related to the hypothetical Fethiye–Burdur fault zone, a correlation previously suggested by several authors (e.g., Taymaz and Price, 1992; Barka et al., 1997; Temiz et al., 1997).

Numerous N20°E bathymetric trends are evident in the continental slope south and east of Rhodes and between Rhodes and Turkey. The absence of these structures in the Quaternary Rhodes Basin corroborates observations from mainland Rhodes that the N20°E-striking faults are older than the N70°E-striking ones, which mark the onset of a new deformation phase during which the forearc underwent significant morphological and kinematic reorganization (ten Veen and Kleinspehn, 2002).

4.7. The Great Slide

Woodside et al. (1998) recognized the Great Slide as an extensive (~2200 km^2) and voluminous (~550 km^3) multilobe, north- and southwestward-flowing debris-flow unit. It originated between the Anaximander and Anaximenes mountains, leaving a huge depression where the Plio–Quaternary sediment is missing (Fig. 2A). Along its northern rim, at least three lobes are distinguishable. Its big western lobe appears detached from its main body along a NNE–SSW-trending scarp. This may well represent a secondary escarpment within the body of this debris flow, thus indicating continuous instability, possibly induced by a buried N20°E-striking fault. Diapiric zones of seismic wipe-out may indicate the occurrence of gas venting and/or upward fluid release (Fig. 6). These processes may have caused surface sediment instability, leading to the creation of the small lobe deposited in the central front of the Great Slide between its huge western and eastern lobes. Slopes at the toe of this slide (Fig. 2A) are steep, reaching up to 10°, indicating that this slide is still active or became inactive only recently.

Internally, the Great Slide has a chaotic structure, with severely folded and/or faulted strata. Fig. 9 shows that sections with strong sub-seafloor reflectors have seismic wipe-outs beneath them and are often associated with bathymetric depressions. Deep-tow side-scan sonar (Fig. 10) shows that these depressions either represent circular pockmarks or linear gullies. The observed strong difference in seismic velocity suggests the presence of gas in these sediments, and the seismic voids reaching the seafloor further suggest the presence of seafloor vents (Woodside et al., 1998). Although it is plausible that faulting underneath the Great Slide facilitated gas release, its disorganized structural patterns are not indicative of regional crustal deformation but instead by dewatering and degassing of this unstable slide mass. Another example of degassing and dewatering through the Great Slide is provided by the Anthill (Fig. 2) along the eastern limit of its western lobe. This hill rises 800 m above the surrounding seafloor and is characterized by exceptionally high sediment thickness and accumulation rates (0.12 m/kyr), suggesting extra sediment supply by ejection of sediment from within the core of the hill (Woodside et al., 1997).

We speculate that this western mountainous area as a whole has been uplifted due to the interaction of the N20°E- and N70°E-trending faults (see above), and in the recent past, a fault-controlled area collapsed between what are nowadays the Anaximander *s.s.* and Anaximenes mountains. Both these mountains have a considerable thickness of Plio–Quaternary (PQ) sediment (Anaximander as a whole and Anaximenes only in its western part). Such elevated sediment packages are expected to have the tendency to be unstable, especially with high gas content as may be the case here (Woodside et al., 1998). The Great Slide can thus be regarded as the expression of such instability and the mountains are the remnants. The curved northern slope of the Anaximenes Mountain is such a remnant, which is not related to one fault but rather to a combination of N20°E- and N70°E-striking faults. Note also that these faults (especially the N20°E-striking set) have considerable vertical displacements, juxtaposing unit PQ and acoustic basement (see Fig. 9). We suggest that this fault-controlled lithological contrast is employed as a detachment level for the Great Slide. The slope steepening necessary for the initiation of the Great Slide may have been induced by the (re-)activation of the N120°E-striking strike-slip faults SW of the Anaximander Mountain *s.s.* and/or by the progressive deepening of the Finike Basin to the north, which is controlled by N70°E-striking strike-slip faults.

5. Neotectonic development

Based on the presented results of surface mapping and vertical seismic reflection data, we can establish the sequence of tectonic events that led to the development of the Anaximander Mountains in relation to plate-boundary processes at the junction of the Hellenic and Cyprus arcs. As syn-depositional deformation of basin fill has been often used to assign activity to faults and fault zones, it should be noted that the precision of the presented tectonostratigraphy would be improved by better dating of the deep marine basin fill on and around the Anaximander Mountains. In spite of these limitations, we present a relative tectonostratigraphy which describes the multiphase development of the western and eastern mountains (Fig. 11).

5.1. Phase 1

During progressive folding related to the advance of the Lycian Nappes, the protruding flysch deposits of the Lower–Middle Miocene MF unit lapped onto the evolving anticlinal structures and are mainly preserved in the synclines. At some time around the Serravallian–Tortonian transition, the Bey Dağları anticline must have become affected by extension on N120°E-striking normal faults, oriented perpendicular to the fold trend. Differential vertical motions generated graben structures, which preserved the Early–Middle Miocene flysch deposits (the MF unit). Kissel and Poison (1987) measured a Middle Miocene 30° anticlockwise rotation of the Bey Dağları, related to the emplacement of the Lycian Nappes. As no younger palaeomagnetic rotations occurred, we can assume that the Late Miocene N120°E-striking faults retain their original orientation. This initial neotectonic period of extensional faulting will be designated as phase 1.

Like in the onshore Kaşaba Graben, Serravallian–Tortonian deposits are absent in the Anaximander Mountains, suggesting that the N120°E-striking grabens were subaerial basins without major drainage. However, in the Isparta Angle to the east, Tortonian deltaic and reefal deposits are unconformably overlain by Pliocene marine deposits (Glover and Robertson, 1998), testifying to the occurrence of a regional latest Miocene unconformity. As previously discussed, the absence of Messinian deposits in the Rhodes Basin (Woodside et al., 2000) indicates that this area was also continental or shallow marine until this time. We thus infer that in the late Middle Miocene and early Late Miocene (Serravallian–Tortonian), a vast area of subaerial to shallow marine grabens existed across the southern Aegean (e.g., Crete; ten Veen and Postma, 1999), through Rhodes (ten Veen and Kleinspehn, 2002), to SW Turkey and the present-day Anaximander Mountains.

Although no MF unit could be recognized on the Anaxagoras Mountain, the presence of N120°E-trending faults, fissures and lineaments suggests that these Serravallian–Tortonian basins even reached this area. A major N120°E-trending lineament, which

Age	West (Anaximander, Anaximenes)			East (Anaxagoras)		
	strike	tectonics	fault system	strike	tectonics	fault system
Quaternary	070° + 020°	sinistral strike-slip + normal faulting, strong differential uplift Rock fall and mass-flows	I-33 to I-36, Fig. 8 I-23 to I-26, Fig. 9 all II-group faults	150° + 050-060°	normal and/or oblique faulting + penetrative sinistral strike-slip faulting	III-6, III-18 + II-18, II-19, Fig. 8
Pliocene	120°	local dextral srtike-slip faulting Initation of Great Slide	IV-2, IV-3, Fig. 7	N-S to 010°	secondary? normal faulting	all V-group faults, Fig. 8
Messinian	020°	normal faulting and onset of PQ deposition	II-3, Fig. 3 "Kaş Graben" I-17 to I-19, Figs. 5 and 7 I-14 to I-16, Fig. 6		?	
	Hiatus (no datable deformation due to absence of basin fill)					
Tortonian	Aksu thrust phase					
Serravallian	120°	normal? faulting with tilt-block halfgraben and southward onlap of MF unit on Anaximander Mt.	IV-0, IV-1, Fig. 5 IV-4 to IV-7, Fig. 9		?	
Mesozoic to Early - Middle Miocene	Emplacement of Lycian Nappes					

Fig. 11. Tectonostratigraphy of the Anaximander Mountains comparing the multiphase development of the western and eastern mountains.

could not be recognized as a fault in the seismic lines but which correlates with the N120°E-trending basement ridge south of the Kaş graben, supports the idea of long elongated basins. No reactivation of this N120°E-striking fault zone is evident in later periods.

The development of these N120°E-trending grabens is analogous to the Late Miocene (pre-Messinian) development of Rhodes, which was dominated by N120°E–N130°E-trending subaerial grabens that formed under NE–SW extension (ten Veen and Kleinspehn, 2002). This NE–SW extension was interpreted as a response to Late Miocene southward migration of the Hellenic forearc and lengthening of the plate boundary as its curvature increased from a nearly east–west Middle Miocene plate margin.

5.2. Phase 2 west

After the brief mid-Tortonian Aksu thrust phase, a second phase of extension is marked by the onset of N20°E-striking normal faults and the formation of associated elongated basins, of which the Kaş Graben is a well-preserved example. This phase of basin formation thus starts after the Tortonian and has continued until the present day. Given the absence of Messinian sediment (including evaporites) in the offshore study area, it is difficult to make inferences about precisely when this second extension phase started. The N20°-striking eastern boundary faults of these grabens have been displaced by N70°E-striking sinistral strike-slip faults. We found that both the N70°E- and N20°E-striking fault sets are younger than the onlap of units MF and PQ onto the Anaximander Mountain *s.s*, implying that their initiation was relatively young and similar in age. We thus interpret these N20°E-striking normal faults as marking the onset stage of phase 2, which is characterized by the progressive development of sinistral shear directed towards N70°E. A similar sequence of fault development emerged in various transtension experiments (e.g., Tron and Brun, 1991; Smith and Durney, 1992). Once the sense of shear is developed completely, both normal faulting (on faults striking N20°E) and strike-slip faulting (on faults striking N70°E) thus occur. By analogy with the Bey Dağları in SW Turkey (Kissel and Poison, 1987), we assume no paleomagnetic rotation during the Pliocene–Quaternary period.

Deep marine basins, such as the Finike and Rhodes Basins, developed during this phase due to rapid subsidence of areas that were originally shallow (see above). Judging from the thick sequence of the PQ unit on top of their summits, we infer that the present-day submarine mountains are uplifted parts of former Pliocene–Quaternary deep marine basins (see, e.g., Fig. 5). This phase of young, rapid differential vertical motions is revealed by the comparable thicknesses of the PQ unit both in the Finike Basin and on the Anaximander Mountain *s.s.*. The development of this differential relief creates a potential for the mass flow of the PQ unit from these mountains, as expressed by the Great Slide.

In the SE Rhodes basin, which is separated from the Anaximander Mountains by the West Anaximander Ridge, the fault pattern is highly complex, with N120°E-, N70°E- and N20°E-striking faults. Both the N120°E- and N70°E-striking fault sets are of Plio–Quaternary age and have been active later than the N20°E-striking faults. The regional stress field may thus be the same north and south of the West Anaximander Ridge, but that the existence of older N120°E-striking faults with a favourable orientation to this stress field complicates the strain pattern. With N70°E-striking strike-slip fault zones representing the dominant or principal (sinistral) shear along the eastern branch of the Hellenic Arc (e.g., ten Veen and Kleinspehn, 2002), the N120°E-striking faults may well represent dextral fault zones, consistent with the orientation of the associated pull-apart structures.

5.3. Phase 2 east

The mid-Tortonian Aksu phase was the final phase of episodic westward emplacement that formed the imbricated stack of thrust sheets known as the Antalya Nappe Complex. This Aksu thrusting phase was thus younger than the development of the N120°E-trending grabens and was associated with an important kinematic change in the western mountains that marked the onset of phase 2. Paleomagnetic measurements from the Antalya Basin (within the Antalya Nappe Complex) reveal no vertical-axis rotation since the Early Miocene (Kissel and Poison, 1986). It is thus assumed that structures in the Anaxagoras Mountain, like those in the southern part of the Antalya Nappe Complex, retain their original orientations.

Both westward and southwestward transport of thrust sheets occurred during the Aksu phase (Frizon de Lamotte et al., 1995). Although both these directions can be observed in the northern Bey Dağları, their southernmost part (Susuz Dağ) only indicates the SW direction, suggesting a progressive change in transport direction. This general sense of thrusting is also revealed by the curved NNW–SSE elongation of the Antalya Nappe Complex/Anaxagoras Mountain domain and by the many similarly trending structural features within it. Not all structures in the Antalya Nappe Complex and Anaxagoras Mountain represent thrust faults; some indicate normal or oblique slip faults as well. Plausibly, the thrust faults were reactivated as extensional faults during the post-Aksu period, as has also been deduced from multiple overprinting of faults in the Isparta Angle (Glover and Robertson, 1998). The orientations of these younger extensional faults are thus directly related to the sense of thrusting during the Aksu phase. Whereas the coast west of Antalya Bay is dominated by major north-striking normal faults that have been active during the Pliocene and Quaternary (Glover and Robertson, 1998), faults that strike N150°E, which are common in the Anaxagoras Mountain, are of less importance here. This difference attests to a N–S structural transition, probably reflecting the structural grain and the change in the sense of thrusting of the Anatalya nappes (from E–W in the north to NE–SW in the south).

Both N70°E- and N150°E-striking fault sets are present in the Anaxagoras Mountain and both are active at present (phase 2), given the close relationship between bathymetric steps and deformation of the PQ unit. Apart from some secondary N–S-striking extensional faults, major N20°E-striking extension-related structures are absent.

6. Pliocene–Quaternary regional geodynamics: the enigma solved?

6.1. Relative plate motions and the position of the plate boundary

The Pliocene–Quaternary deformation in the Anaxagoras Mountain *s.l.*, in close proximity to the junction of the Hellenic and Cyprus arcs, is most likely controlled by stresses exerted by relative plate motions. We thus present a model that compares our observations of strain patterns against predicted relative plate motions, based on recent GPS measurements of crustal motions in the eastern Mediterranean (McClusky et al., 2000). The horizontal displacement field for the Aegean–Anatolian platelet was calculated using the McClusky et al. (2000) dataset. Using their original data, a velocity field with 20′ grid spacing was calculated. In the absence of suitable GPS data from the African continent, we adopt velocity estimates from the NUVEL-1A model (DeMets et al., 1994) with the same grid spacing as for the Aegean–Anatolian plate. The motion of the Arabian plate was determined using the newly calculated Euler vector of Westaway (2004, this volume). These velocity fields relative to Eurasia are shown in Fig. 12A.

To study the effects of these relative plate motions, it is first important to establish where the African and Eurasian plates interact (i.e., where to

Fig. 12. (A) Present-day plate motions relative to a stable Eurasia with African plate motion from the NUVEL-1A plate motion solution (DeMets et al., 1994), Arabian plate motion from the new Euler vector calculated by Westaway (2004, this volume), and Anatolian–Aegean rotation field calculated from GPS measurements by McClusky et al. (2000) with the Euler pole for the motion of Anatolia relative to Eurasia denoted by a cross. See text for description of the methods applied. EU, AF, AR and AN denote the Eurasian, African and Arabian plates and the Anatolian platelet. Stippled area represents an ~250 km broad zone in the eastern Hellenic forearc, which takes up distributed deformation that is governed by strain partitioning associated with the oblique subduction of the relatively shallow-dipping African plate (see text for discussion). Heavy black lines denote major, strike-slip dominated plate boundaries; black toothed lines denote convergent plate boundaries (i.e., the active deformation front); grey toothed lines denote Mediterranean Ridge backstop thrust; thin black lines denote strike-slip zones internal to the Hellenic forearc. (B) Relative motions of Anatolia and Arabia at their boundaries with the African plate are calculated from displacement fields shown in (A). The calculated Euler pole for the motion of Anatolia relative to Africa is 30.5°N, 37.9°E, 1.12° Myr^{-1} and denoted by cross. AM denotes the Anaximander Mountains. ESM denotes the Erastosthenes "Seamount". (C) Interpretative model of the observed present-day deformation related to rapidly changing relative plate motion at the junction between the Hellenic and Cyprus arcs, summarizing our interpretation. White open arrows denote calculated relative plate motions; wavy double lines indicate areas of compression. Deformation zones in the Mediterranean Ridge (MR) are taken from Huguen et al. (2001).

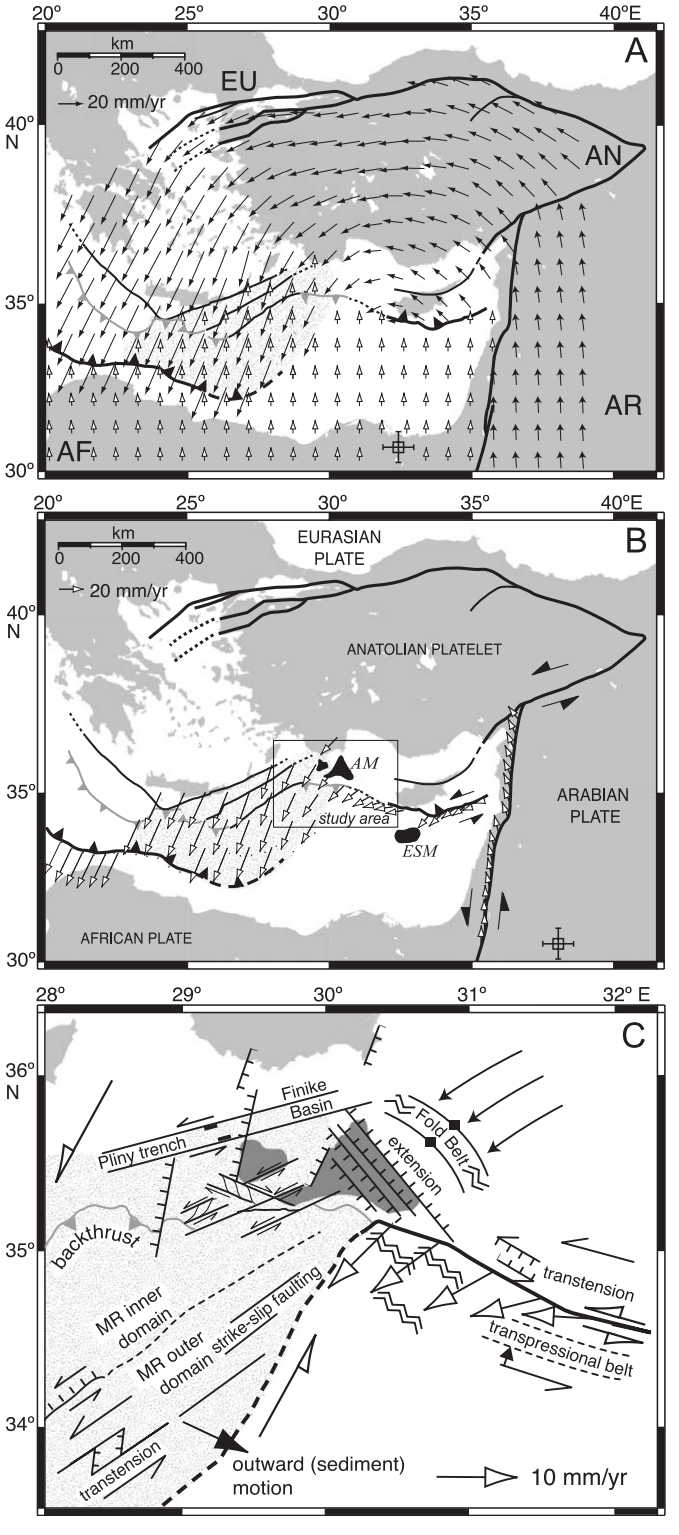
20°
25°
30°
35°
40°E
A
km
0
200
400
20 mm/yr
EU
AN
AR
AF
40°
N
35°
30°
B
EURASIAN
PLATE
ANATOLIAN PLATELET
AM
study area
ESM
ARABIAN
PLATE
AFRICAN PLATE
28°
29°
30°
31°
32° E
C
36°
N
35°
34°
Finike
Basin
Pliny trench
Fold Belt
extension
backthrust
MR inner
domain
MR outer
domain
strike-slip faulting
transtension
transpressional belt
outward (sediment)
motion
10 mm/yr

position a meaningful plate boundary). Previous studies that have applied the GPS velocity field to predict relative plate motions (e.g., Kahle et al., 1998; Kahle et al., 2000; McClusky et al., 2000) placed this plate boundary along the Hellenic and Strabo "trenches", which were originally thought to represent the active subduction zone (e.g., McKenzie, 1970). Because it is now known that these "trenches" are not part of the subduction zone but instead coincide with the backthrust of the MR accretionary prism (e.g.,Chaumillon and Mascle, 1997; Huguen et al., 2001), the actual plate boundary should be located elsewhere. In the case of head-on subduction, the plate boundary would theoretically lie at the contact between the Mediterranean Ridge accretionary prism and the subducting African plate, i.e., at the Mediterranean Ridge deformation front. In such a case, the deformation front is the interface that is most critical in determining the geodynamic interaction between the two plates. This situation may apply to the western Hellenic subduction zone, where subduction is approximately perpendicular to the Mediterranean Ridge deformation front (Fig. 12B), although we will not elaborate on this part because it is peripheral to understanding the geodynamics of the Anaximander Mountains. In the eastern Mediterranean Ridge, Huguen et al. (2001) explained that important strike-slip fault zones reflect strain partitioning related to oblique subduction, which also facilitated lateral escape of the sediment cover. In addition, the Pliny and Strabo "trenches", cutting the Hellenic forearc, are also believed to result from sinistral transform motions caused by the obliquity of relative plate motion (e.g., Le Pichon et al., 1979; Huchon et al., 1982). Even further inland on Crete and Rhodes, similarly trending sinistral strike-slip faults have been observed, which demonstrate that the effects of relative plate motion also penetrate into the islands of the Hellenic forearc (e.g., ten Veen and Kleinspehn, 2002). Therefore, we suggest that a very broad zone (~250-km wide) exists, which takes up distributed deformation that is governed by the oblique subduction of the relatively shallow-dipping African plate (Fig. 12B). This shallow dip of the African oceanic lithosphere beneath the Mediterranean Ridge was recently demonstrated in a wide-aperture seismic study by Bonhoff et al. (2001). The actual deformation front is the expression of superficial outward sediment flow, which might be facilitated by the oblique subduction, and may also be influenced by decollement along the base of the Messinian evaporates (Huguen et al., 2001).

The absence of an accretionary wedge, a volcanic arc and a pronounced subduction trench along the Cyprus Arc led Woodside et al. (2002) to conclude that no significant subduction takes place here at present. However, seismicity indicates limited underthrusting south of Cyprus, and further north within Antalya Gulf, reveals the unclear presence of a lithospheric slab dipping northeastward beneath this arc (e.g., Rotstein and Kafka, 1982; Papazachos and Papaioannou, 1999). Despite the absence of clear subduction, the relative plate motion in this region is consistent with the calculations presented in Fig. 12B.

6.2. Geodynamic model for the Anaximander Mountains

The relative plate motion vectors at the assumed plate boundary (Fig. 12B) predict that the Hellenic plate boundary is moving SW as extension of the Aegean–Western Turkey domain proceeds. The eastern Cyprus Arc experiences overall northwestward retreat. The transition between these two arc segments lies in the vicinity of the Anaximander Mountain region, an area characterized by rapidly changing relative plate motions that are explained by close proximity to the pole of rotation of the Anatolian platelet relative to the African plate (Fig. 12B, locality after McClusky et al., 2000).

Based on comparison of plate boundary orientation and predicted relative plate motions, we infer that the western Cyprus Arc (the Florence Rise) is characterized by sinistral strike-slip but that the strike-slip component decreases towards the Anaximander Mountains due to a decrease in the tangential component of relative plate motion (i.e., an increase in arc-normal compression; Fig. 12C). Fault plane solutions for the few significant earthquakes that have occurred along the Florence Rise SW of Cyprus (Papazachos and Papaioannou, 1999) have maximum instantaneous shortening axes parallel to our predicted plate motion vector (Θ_P=0°). Teyssier et al. (1995) proposed kinematic models

describing the relationship between the angle of relative plate motion (α), the orientations of minimum and maximum instantaneous strain axes in the horizontal plane (Θ_T and Θ_P) and the degree of strike-slip partitioning. For the southernmost Florence Rise, with $\Theta_P \approx 0^\circ$ and $\alpha \approx 5^\circ$, these models predict that no strike-slip partitioning occurs (i.e., deformation associated with the relative plate motion occurs only as strike-slip faulting parallel to the plate boundary). This is exemplified by a broad diffuse zone of deformation with parallel strike-slip faults at the Florence Rise (Fig. 12C; Woodside et al., 2002).

Near the Anaximander Mountains, no significant earthquakes occur, and we thus cannot speculate on the degree of strike-slip partitioning. However, the rising seafloor topography between the Florence Rise and the Anaximander Mountains may reflect the increase in arc-normal compression. The absence of horizontal displacement suggests that no significant strike-slip occurs on the S30°E-striking faults in the Anaxagoras Mountain and that these faults are most probably oblique normal faults with a minor sinistral slip component.

For the overriding plate, this implies a transition from pure strike-slip faulting along the southern Florence Rise to almost head-on compression close to the junction of the Hellenic and Cyprus arcs. South of the Florence Rise, Woodside et al. (2002) showed the presence of a zone of transpressional deformation, as can be expected in between areas of compression and pure strike-slip, to the north and south respectively. Near the Anaxagoras Mountain, the GPS data show a general westward increase in velocity towards the southwest (McClusky et al., 2000; Fig. 12A), such that not only is the plate boundary expected to move southwestwards but also arc-normal extension is occurring in the forearc region. This situation is comparable to the arc-normal extension in the Hellenic forearc due to southward migration of the Hellenic subduction zone (ten Veen and Meijer, 1998). These ideas fit well with the proposed active extension in the Anaxagoras Mountains. The fold belt east of the Anaxagoras Mountain marks the line across which the relative plate motion starts to increase (Fig. 12A), suggesting that compression can prevail farther east (Fig. 12C). Such perturbations in the velocity field may have caused other rapid changes of deformation style within the Aegean–Anatolian plate.

The angle of convergence beneath the Mediterranean Ridge and the eastern Hellenic forearc does not change significantly (Fig. 12B), so that we anticipate a rather uniform type of transform deformation for the area under consideration. Papazachos et al. (2000) noted several deep transpressional strike-slip earthquakes along the eastern Hellenic Arc, which confirm transform faulting along the subduction interface. It is noteworthy, however, that a misfit exists between the predicted shear direction based on relative plate motions and the observed shear zones, which all strike between N50°E and N70°E (Fig. 12C). This misfit implies that part of the deformation associated with the relative plate motion must be expressed by another sense of deformation, oriented at a high angle to these strike-slip fault zones. The ESE outward growth of the eastern Hellenic forearc and possibly the outward sediment movement in the Mediterranean Ridge may point to partitioning of the strain associated with NNE–SSW shear along the plate boundary. This scenario has also been deduced from the Pliocene–Quaternary kinematics on Rhodes (ten Veen and Kleinspehn, 2002).

We infer that at the latest Miocene–Early Pliocene start of the westward motion of Anatolia and the ensuing SW motion of the Hellenic forearc (i.e., when the strike-slip zones initiated), no strain partitioning occurred and relative plate motions in the eastern Hellenic Arc were taken up by the sinistral strike-slip faults. During continued southwest- and outward motion of the Hellenic Arc, the azimuth of relative plate motion changed such that its obliquity increased. This increase in plate convergence obliquity and the rotation of motion vectors within the Aegean–Anatolian plate did not result in the development of new shear zones but in the addition of a WNW–ESE extensional component. Within the Mediterranean Ridge, Huguen et al. (2001) demonstrated the existence of N50°E-striking transtensional fault zones with associated pull-apart basins, which possibly reflect tensional stresses at an angle to the main shear direction. Although the N70°E-striking sinistral shear zones of the eastern Hellenic Arc penetrate as far as the Anaxagoras Mountain and segment the N150°E-striking faults,

they are not observed farther east. The horizontal slip on these shear zones evidently decreases eastward, given that these N150°E-striking faults have not been laterally displaced.

Because the orientation and position of the plate boundary, and thus the sense of relative plate convergence, have changed with time (ten Veen and Kleinspehn, 2002) a steady-state model does not apply to this region. This is exemplified by the tectonostratigraphy of the Anaximander Mountains, which reveals at least two neotectonic phases. The first, Serravallian–Tortonian, phase is characterized by NNE–SSW extension whereas the second, Messinian–Quaternary, phase is governed by major N70°E-striking strike-slip faulting. At a higher level of detail, the continuously changing stress field has been reflected in the evolution of this second phase, which started with N20°E-striking normal faulting, followed by N70°E-striking sinistral strike-slip faulting. In the eastern Anaximander Mountains, few new faults were initiated, but preexisting thrust faults that had developed during the Aksu phase of nappe emplacement were most likely reactivated as (oblique) normal faults. On a larger scale, this late phase of thrusting, which we suggest is related to the onset of the westward motion of Anatolia, must have determined the orientation of the western Cyprus Arc, including the present-day Florence Rise.

7. Conclusions

We establish the sequence of tectonic events related to plate-boundary processes at the junction of the Hellenic and Cyprus arcs:

(1) The western mountains in this region (Anaximander and Anaximenes) correlate with the neritic limestones of the Bey Dağları unit of SW Turkey, whereas the eastern Anaxagoras Mountain is a continuation of the ophiolitic Antalya Nappe Complex. This lithological contrast is also shown in gravimetry, denoting a deep-seated crustal difference.

(2) During the Serravallian and Tortonian, an array of relatively simple N120°-trending grabens developed in a vast continental region throughout the southern Aegean and SW Turkey.

(3) A kinematic change in the latest Miocene, related to the onset of the westward motion of Anatolia, marked the start of differential subsidence that resulted in the formation of the Anaximander Mountains and which is marked by a regional unconformity between Lower–Middle Miocene and Plio–Quaternary sedimentary units.

(4) Post-Tortonian (Messinian–Quaternary) deformation of the western mountains is characterized by N70°E-directed sinistral shear, which is marked by the onset of N20°E-striking normal faulting that generated long graben-like depressions. During the Pliocene, these basins were transected by N70°E-trending sinistral shear zones, although continued crustal extension indicates deformation in transtension. The eastern mountains are characterized by N150°E-trending dextral oblique/normal fault zones that lack evidence of significant strike-slip motion.

(5) The Pliny “trench” does not connect with the hypothetical onshore Fethiye–Burdur fault zone but instead with the offshore Finike Basin, forming a very long and broad zone of deformation.

(6) The predicted sense and rate of relative motion between the African plate and the Anatolian platelet change abruptly in the vicinity of the junction between the Hellenic and Cyprus Arcs because of its close proximity to the Euler pole for this relative motion. These predictions indicate that along both the eastern Hellenic Arc and the western Cyprus Arc (the Florence Rice), this relative motion has a sinistral sense. As far as deformation in the upper plate is concerned, the southern Florence Rise is characterized by pure wrench tectonics, whereas moving northward along this plate boundary, the strike-slip component decreases towards the Anaximander Mountains. Here, compression prevails at the plate boundary, whereas the outer-arc domain of the overriding plate is experiencing arc-normal extension related to trench retreat, governed by the westward increase in the southwestward motion of the Aegean–Anatolian plate. At the arc junction, the eastern Hellenic Arc is

experiencing left-lateral faulting in combination with WNW–ESE extension and sediment movement, reflecting both relative plate motion and WNW–ESE outward growth of the eastern Hellenic forearc.

Acknowledgements

This research was supported by the Nederlandse Organisatie voor Wetenschappelijk Onderzoek (NWO) grant no. 831.48.009 to JtV. Data collection and analysis were made possible through other NWO grants: ANAXIPROBE project (NWO no. 750.195.02), MEDINAUT/MEDINETH project (NWO no. 750.199.01) and MediSed (NWO no. 809.63.011). Most of the seismic data were processed during the 1996 Training Through Research expedition (TTR6). Some figures were created using the GMT (Generic Mapping Tools) software, and we are indebted to its authors, P. Wessel and W. Smith, for making it available. André Poisson is thanked for stimulating discussions concerning the geology of SW Turkey. We also thank the reviewers, R. Westaway and E. Demirbağ, for their comments and suggestions to improve this paper. This is contribution no. 20030202 of the Netherlands Research School of Sedimentary Geology.

References

Angelier, J., Lyberis, N., Le Pichon, X., Barrier, E., Huchon, P., 1982. The tectonic development of the Hellenic arc and the Sea of Crete: a synthesis. Tectonophysics 86, 159–196.

Barka, A.A., Reilinger, R., Şaroğlu, F., Şengör, A.M.C., 1997. The Isparta angle, its importance in neotectonics of the eastern Mediterranean region. IESCA-1995 Proceedings 1, 3–17.

Ben-Avraham, Z., Grasso, M., 1991. Crustal structure variations and transcurrent faulting at the eastern and western margins of the eastern Mediterranean. Tectonophysics 196, 269–278.

Biju-Duval, B., Letouzey, J., Montadert, L., Courrier, P., Mugniot, J.F., Sancho, J., 1974. Geology of the Mediterranean sea basins. In: Burke, C.A., Drake, C.L. (Eds.), The Geology of Continental Margins. Springer-Verlag, Berlin, pp. 695–721.

Blumenthal, M.M., 1963. Le système structural du Taurus sud Anatolies. Bull. Soc. Géol. Fr. Livre à Mémoire de Professor P. Fallot, Mémoir hors-série, vol. 1, pp. 611–662.

Bonhoff, M., Makris, J., Papanikolaou, D., Stavrakakis, G., 2001. Crustal investigation of the Hellenic subduction zone using wide aperture seismic data. Tectonophysics 343, 239–262.

Brunn, J.H., Dumont, J.F., de Graciansky, P.C., Gutnic, P.C., Juteau, Th., Marcoux, J., Monod, O., Poisson, A., 1971. Outline of the geology of the western Taurids. In: Campbell, A.S. (Ed.), Geology and History of Turkey. Petrol. Expl. Soc., Libya, pp. 225–255.

Chaumillon, E., Mascle, J., 1997. From foreland to forearc domains: New multichannel seismic reflection survey of the Mediterranean ridge accretionary complex (Eastern Mediterranean). Mar. Geol. 138, 237–259.

DeMets, C., Gordon, R., Argus, D., Stein, S., 1994. Current plate motions. Geophys. J. Int. 101, 425–478.

Frizon de Lamotte, D., Poisson, A., Auborg, C., Temiz, H., 1995. Chevauchements post-tortoniens vers l'ouest puis vers le sud au coeur de l'angle d'Isparta (Taurus Turquie). Consequences géodynamique. Bull. Soc. Géol. Fr. 166 (1), 59–67.

Glover, C., Robertson, A., 1998. Neotectonic intersection of the Aegean and Cyprus tectonic arcs: extensional and strike-slip faulting in the Isparta Angle, SW Turkey. Tectonophysics 298, 103–132.

Gutnic, M., Monod, O., Poisson, A., Dumnont, J.F., 1979. Géologie des Taurides Occidentales (Turquie). Mém. Soc. Géol. Fr. 137, 1–112.

Hayward, A.B., 1984. Miocene clastic sedimentation related to the emplacement of the Lycian Nappes and the Antalya Complex, S.W. Turkey. In: Dixon, J.E., Robertson, A.H.F. (Eds.), The Geological Evolution of the Eastern Mediterranean, Spec. Publ.-Geol. Soc. London, vol. 17, pp. 287–300.

Huchon, P., Lyberis, N., Angelier, J., Le Pichon, X., Renard, V., 1982. Tectonics of the Hellenic Trench, a synthesis of Sea-Beam and submersible obervations. Tectonophysics 86, 69–211.

Huguen, C., Mascle, J., Chaumillon, E., Woodside, J.M., Benkhelil, J., Kopf, A., Volskonkaia, A., 2001. Deformation styles of the eastern Mediterranean Ridge and surroundings from combined swath mapping and seismic reflection profiling. Tectonophysics 343, 21–47.

Ivanov, M.K., Limonov, A.F., Woodside, J.M., 1992. Geological and geophysical investigations in the Mediterranean and Black Seas. Initial results of the 'Training-through-Research' cruise of R/V Gelendzhik in the eastern Mediterranean and the Black Sea (June–July 1991). UNESCO Rep. Mar. Sci. 56. 206 pp.

Kahle, H.G., Straub, C., Reilinger, R., McClusky, S., King, R., Hurst, K., Veis, G., Kastens, K., Cross, P., 1998. The strain rate field in the eastern Mediterranean Region, estimated by repeated GPS measurements. Tectonophysics 294, 237–252.

Kahle, H.G., Cocard, M., Yannick, P., Geiger, A., Reilinger, R., Barka, A., Veis, G., 2000. GPS-derived strain rate fields within the boundary zones of the Eurasian, African and Arabian plates. J. Geophys. Res. 105, 23353–23370.

Kissel, C., Poison, A., 1986. Etude paléomagnétique préliminaire des formations néogonès du basin d'Antalya (Taurides Occidental, Turquie). C. R. Acad. Sci. Paris 302, 711–716.

Kissel, C., Poison, A., 1987. Etude paléomagnétique préliminaire des formations cénozoïques des Bey Daglari (Taurides Occidental, Turquie). C. R. Acad. Sci. Paris 304, 343–348.

Le Pichon, X., Angelier, J., 1979. The Hellenic arc and trench system: a key to the neotectonic evolution of the eastern Mediterranean area. Tectonophysics 60, 1–42.

Le Pichon, X., Aubouin, J., Lybéris, N., Monti, S., Renard, V., Got, H., Hsü, K., Mart, Y., Mascle, J., Matthews, D., Mitropoulos, D., Tsoflias, P., Chronis, G., 1979. From subduction to transform motion: a Seabeam survey of the Hellenic trench system. Earth Planet. Sci. Lett. 44, 441–450.

Le Pichon, X., Chamonrooke, N., Lallemant, S., Noomen, R., Veis, G., 1995. Geodetic determination of the kinematics of central Greece with respect to Europe, implications for eastern Mediterranean tectonics. J. Geophys. Res. 100, 12675–12690.

Martinod, J., Hatzfeld, D., Brun, J.P., Davy, P., Gautier, P., 2000. Continental collision, gravity spreading, and kinematics of Aegea and Anatolia. Tectonics 19, 290–299.

Mascle, J., Le Cleach, A., Jongsma, D., 1986. The eastern Hellenic margin from Crete to Rhodes, example of progressive collision. Mar. Geol. 73, 145–168.

McClusky, S., et al., 2000. Global Positioning System constraints on plate kinematics and dynamics in the eastern Mediterranean and Caucasus. J. Geophys. Res. 105, 5695–5719.

McKenzie, D.P., 1970. The plate motions of the Mediterranean region. Nature 226, 239–243.

MEDINAUTH/MEDINETH Shipboard Scientific Parties, 2000. Linking Mediterranean brine pools and mud volcanism. Eos, Transactions, American Geophysical Union, 81/51, 625, 631–633.

Molnar, P., Tapponier, P., 1975. Cenozoic tectonics of Asia. Science 189, 419–426.

Nesteroff, W.D., Lort, J.M., Angelier, J., Bonneau, M., Poisson, A., 1977. Esquisse structurale en Mediterranée orientale au front de l'arc égéen. In: Biju-Duval, B., Montadert, L. (Eds.), International Symposium on the Structural History of the Mediterranean Basins. Editions Technip, Paris, pp. 241–256.

Nur, A., Ben-Avraham, Z., 1978. The eastern Mediterranean and the Levant, tectonics of continental collision. Tectonophysics 46, 297–311.

Papazachos, B.C., Papaioannou, C.A., 1999. Lithospheric boundaries and plate motions in the Cyprus area. Tectonophysics 308, 193–204.

Papazachos, B.C., Karakostas, V.G., Papazachos, C.B., Scordilis, E.M., 2000. The geometry of the Wadati–Benioff zone and lithospheric kinematics in the Hellenic arc. Tectonophysics 319, 275–300.

Platzman, E.S., Tapırdamaz, C., Sanver, M., 1998. Neogene anticlockwise rotation of central Anatolia (Turkey): preliminary palaeomagnetic and geochronological results. Tectonophysics 299, 175–189.

Poisson, A., 1977. Recherches geologiques dans les Taurides occidentales, PhD thesis, University of Paris–Orsay. 795 pp.

Poisson, A., Akay, E., Dumont, J.F., Uysal, S., 1984. The Isparta Angle, a Mesozoic paleorift in the Western Taurus. In: Tekeli, O., Goncuoğlu, C. (Eds.), International Symposium on the Geology of the Taurus Belt. Spec. Publ. M.T.A, Ankara, pp. 11–26.

Robertson, A.H.F., 1998. Tectonic significance of the Eratosthenes Seamount: a continental fragment in the process of collision with a subduction zone in the eastern Mediterranean (Ocean Drilling Program Leg 160). Tectonophysics 298, 63–82.

Rotstein, Y., Ben-Avraham, Z., 1985. Accretionary processes at subduction zones in the eastern Mediterranean. Tectonophysics 112, 551–561.

Rotstein, Y., Kafka, A.L., 1982. Seismotectonics of the Cyprean Arc, eastern Mediterranean region: subduction, collision and arc jumping. J. Geophys. Res. 87, 7694–7706.

Ryan, W.B.F., Hsü, K., et al., 1973. Initial Reports of the Deep Sea Drilling Project, vol. XIII. US Government Printing Office, Washington, DC. (in two parts), 1447 pp.

Sage, L., Letouzey, J., 1990. Convergence of the African and Eurasian plate in the eastern Mediterranean. In: Letouzey, J. (Ed.), Petroleum and Tectonics in Mobile Belts. Edition Technip, Paris, pp. 49–68.

Smith, J.V., Durney, D.W., 1992. Experimental formation of brittle structural assemblages in oblique divergence. Tectonophysics 216, 235–253.

Taymaz, T., Price, S.P., 1992. The 12.05.1971 Burdur earthquake sequence: a synthesis of seismological and geological observations. Geophys. J. Int. 108, 589–603.

Taymaz, T., Jackson, J., McKenzie, D., 1991. Active tectonics of the north and central Aegean Sea. Geophys. J. Int. 106, 433–490.

Temiz, H., Poisson, A., Andrieux, J., Barka, A., 1997. Kinematics of the Plio–Quaternary Burdur–Dinar cross-fault system in SW Anatolia (Turkey). Ann. Tecton. 11, 102–113.

ten Veen, J.H., Kleinspehn, K.L., 2002. Geodynamics along an increasingly curved convergent plate margin: Late Miocene–Pleistocene Rhodes (Greece). Tectonics 21, doi:10.1029/2001TC001287 (published online).

ten Veen, J.H., Meijer, P.T., 1998. Late Miocene to Recent tectonic evolution of Crete (Greece): geological observations and model analysis. Tectonophysics 298, 191–208.

ten Veen, J.H., Postma, G., 1999. Neogene tectonics and basin fill patterns in the Hellenic outer-arc. Basin Res. 11, 223–241.

Teyssier, C., Tikoff, B., Markley, M., 1995. Oblique plate motion and continental tectonics. Geology 23, 447–450.

Tron, V., Brun, J.P., 1991. Experiments on oblique rift in brittle–ductile systems. Tectonophysics 188, 71–84.

Westaway, R., 2004. Kinematic consistency between the Dead Sea Fault Zone and the Neogene and Quaternary left-lateral faulting in SE Turkey. Tectonophysics 391, 203–237.

Woodside, J.M., 1977. Tectonic elements and crust of the eastern Mediterranean Sea. Mar. Geophys. Res. 3, 317–354.

Woodside, J., Dumont, J.F., 1997. The Anaximander Mountains are a southward rifted and foundered part of the southwestern Turkish Taurus. Terra Nova 9 (Abstr. Suppl. 1), 394.

Woodside, J.M., Limonov, A.F., Ivanov, M.K. (Eds.), 1997. Neotectonics and fluids flow through seafloor sediments in the eastern Mediterranean and Black Sea, Intergovern. Ocean. Comm. Techn. Ser., vol. 48. 226 pp.

Woodside, J.M., Ivanov, M.K., Limonov, A.F., 1998. Shallow gas and gas hydrates in the Anaximander Mountains region, eastern Mediterranean Sea. In: Henriet, J.P., Mienert, J. (Eds.), Gas Hydrates, Relevance to World Margin Stability and Climate Change, Spec. Publ.-Geol. Soc. London, pp. 177–193.

Woodside, J., Mascle, J., Huguen, C., Volkonskaia, A., 2000. The Rhodes Basin, a post-Miocene tectonic trough. Mar. Geol. 165, 1–12.

Woodside, J.M., Mascle, J., Zitter, T.A.C., Limonov, A.F., Ergun, M., Volkonskaia, A., Shipboard scientists of the PRISMED II expedition, 2002. The Florence Rise, the western bend of the Cyprus Arc. Mar. Geol. 185, 177–194.

Wortel, M.J.R., Spakman, W., 1992. Structure and dynamics of subducted lithosphere in the Mediterranean region. Proceedings Koninklijke Nederlandse Akademie van Wetenschappen, 95, 325–347.

Zitter, T.A.C., Woodside, J.M., Mascle, J., 2003. The Anaximander Mountains: a clue to the tectonics of southwest Anatolia. Geol. J. 38, 375–394.